DLR-IB-FT-BS-2021-253

Analysis and comparison of the performance of satellite navigation procedures from flight test data at Zurich Airport

Interner Bericht
Hochschulschrift

Autor: Cesario Bergamin, Zeshan Khan

Deutsches Zentrum
DLR für Luft- und Raumfahrt

Institutsbericht
IB 111-2021/253

Analysis and comparison of the performance of satellite navigation procedures from flight test data at Zurich Airport

Cesario Bergamin
Zeshan Khan

Institut für Flugsystemtechnik
Braunschweig

059 Seiten
029 Abbildungen
006 Tabellen
033 Referenzen

Deutsches Zentrum für Luft- und Raumfahrt e.V.
Institut für Flugsystemtechnik
Abteilung Flugdynamik und Simulation

Braunschweig, den 04.01.2021

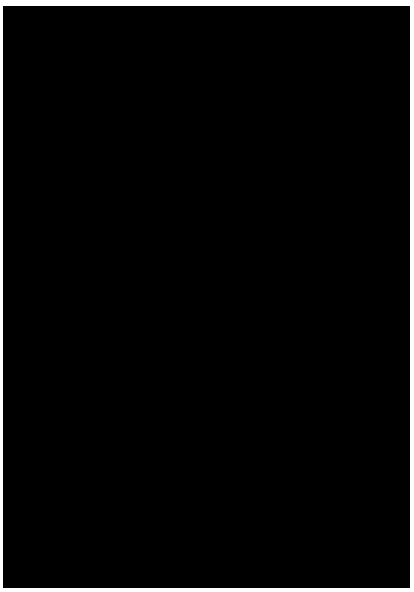

Institutsdirektor:	Prof. Dr.-Ing. S. Levedag
Abteilungsleiter:	Dr.-Ing. H. Duda
Betreuer:	Dr.-Ing. F. Abdelmoula
Verfasser:	Cesario Bergamin Zeshan Khan

Zürcher Hochschule
für Angewandte Wissenschaften

School of Engineering

ZAV Zentrum für Aviatik

DLR Deutsches Zentrum für Luft- und Raumfahrt

Projektarbeit (Aviatik)

Analysis and comparison of the performance of satellite navigation procedures from flight test data at Zurich Airport

Autoren	Cesario Bergamin Zeshan Khan
Hauptbetreuung	Dr. Michael Felux
Industriepartner	Deutsches Zentrum für Luft- und Raumfahrt (DLR)
Externe Betreuung	Dr. Fethi Abdelmoula
Datum	18. Dezember 2020

Erklärung betreffend das selbstständige Verfassen einer Bachelorarbeit an der School of Engineering

Mit der Abgabe dieser Bachelorarbeit versichert der/die Studierende, dass er/sie die Arbeit selbständig und ohne fremde Hilfe verfasst hat. (Bei Gruppenarbeiten gelten die Leistungen der übrigen Gruppenmitglieder nicht als fremde Hilfe.)
Der/die unterzeichnende Studierende erklärt, dass alle zitierten Quellen (auch Internetseiten) im Text oder Anhang korrekt nachgewiesen sind, d.h. dass die Bachelorarbeit keine Plagiate enthält, also keine Teile, die teilweise oder vollständig aus einem fremden Text oder einer fremden Arbeit unter Vorgabe der eigenen Urheberschaft bzw. ohne Quellenangabe übernommen worden sind.

Bei Verfehlungen aller Art treten die Paragraphen 39 und 40 (Unredlichkeit und Verfahren bei Unredlichkeit) der ZHAW Prüfungsordnung sowie die Bestimmungen der Disziplinarmassnahmen der Hochschulordnung in Kraft.

Ort, Datum:	**Name Studierende:**
18.12.2020, Zürich	Cesario Bergamin [redacted]
18.12.2020, Zürich	Zeshan Khan

Acknowledgements

The authors would like to thank Dr. Pascal Truffer from skyguide for his support in providing the GBAS data from the GBAS at Zurich Airport, Dr. Fethi Abdelmoula and Dr. Simona Circiu from the German Aerospace Center (DLR) for the provision of the flight test data and the support with data processing, and Mr. Natali Cacciopoli from the Eurocontrol Pegasus team for his support with the Pegasus tool and data processing.

Zusammenfassung

In dieser Arbeit wird die Performance von Standalone-Signalen globaler Navigationssatellitensysteme (GNSS) und von Signalen, die durch ein Ground Based Augmentation System (GBAS) korrigiert werden, verglichen. Dieser Vergleich erfolgt durch die Untersuchung von Flugtestdaten, die vom Deutschen Zentrum für Luft- und Raumfahrt (DLR) und Skyguide am internationalen Flughafen Zürich (LSZH) gesammelt wurden. Damit wird die Betriebsfähigkeit der GBAS-Station am LSZH bewertet und eine Aussage zu ihrer differentiellen Augmentationsleistung getroffen.

Eine kurze Diskussion des derzeit am LSZH eingesetzten Instrumentenlandesystems (ILS) zeigt dessen Limitationen auf und liefert eine Motivation für den Einsatz einer hochwertigen, modernen Präzisionsanflugführung wie dem GBAS.

Dieser Diskussion folgt ein Überblick über GNSS mit seinen Kernkonstellationen und dem Funktionsprinzip der Standalone GNSS-Positionslösung, sowie eine Beschreibung der für die Positionslösung verwendeten GNSS-Signale. Dies bildet die Grundlage für die Funktionsweise von GBAS.

Im nächsten Kapitel werden die Fehlerquellen erläutert, die die Leistung der GNSS-Signale negativ beeinflussen. Diese Beeinträchtigungen führen zu einer Ungenauigkeit der Standalone GNSS-Signale und somit können die Anforderungen an eine präzise Anflugführung nicht erfüllt werden. Daraus erklärt sich die Notwendigkeit eines differenziell korrigierten Augmentierungssystems, um eine für Präzisionsanflüge ausreichende Performance zu erreichen.

Schließlich wird der Zweck eines GBAS-Landesystems (GLS) erörtert und dessen Infrastruktur, bestehend aus einem Boden- und einem Flugzeug-Subsystem, unter Berücksichtigung der von jedem Subsystem durchgeführten Korrekturerzeugung erläutert. Darüber hinaus werden die GBAS-Leistungsmerkmale, bestehend aus Genauigkeit, Integrität, Kontinuität und Verfügbarkeit, das Hauptziel eines GBAS-Systems aufzeigen und die Funktionalität hinter der Fähigkeit, die vordefinierten Leistungsanforderungen zu erfüllen, erklären.

Schließlich werden die Flugtestdaten untersucht, indem zunächst die Flugbahn des durchgeführten Testfluges visualisiert wird. Dann wird das für die Berechnung der Positionslösung verwendete Programm PEGASUS diskutiert, gefolgt von einer Analyse der Genauigkeit von Standalone-Signalen auf die Positionslösung einer GBAS-Referenzantenne. Die Flugpfade basierend auf Standalone- und GBAS-korrigierten Positionslösungen werden verglichen und die Protection Levels, die die Integrität von GBAS definieren, werden diskutiert. Darüber hinaus wird der Grund für Peaks in den Protection Levels erklärt, indem die verwendete Satellitengeometrie während dieser Peaks betrachtet wird. Abschließend werden die Protection Levels mit den Alert Limits verglichen und der Unterschied zwischen der Standalone- und der GBAS-korrigierten Positionslösung wird analysiert.

Abstract

In this work, the performance of standalone signals by Global Navigation Satellite Systems (GNSS) and signals augmented by an operational Ground Based Augmentation System (GBAS) is compared. This comparison is done by investigating flight test data gathered at Zurich International Airport (LSZH) by the German Aerospace Center (DLR) and Skyguide. Thus, the operational capability of the GBAS station at LSZH is evaluated and a statement to its differential augmentation performance is made.

A short discussion of the currently at LSZH used Instrument Landing System (ILS) reveals its limitations, providing a motivation for the use of a more sophisticated, state-of-the-art precision approach guidance such as the GBAS.

This discussion is followed by an overview of GNSS with its core constellations and the operating principle of standalone GNSS positioning service, as well as a description of the GNSS signals used for positioning service. This provides the base for the functionality of GBAS.

The next chapter explains the error sources that adversely influence the performance of GNSS signals. These impairments lead to inaccuracy of standalone GNSS signals and thus, requirements for precision approach guidance cannot be complied with. This explains the necessity of a differentially corrected augmentation system in order to reach a performance sufficient enough for precision approaches.

Eventually, the purpose of a GBAS Landing System (GLS) is discussed and its infrastructure, consisting of a ground and aircraft subsystem, are elucidated by taking into account the correction generation done by each subsystem. Furthermore, the GBAS Performance Characteristics, comprised by the Accuracy, Integrity, Continuity and Availability reveal the main goal of a GBAS system and explains the functionality behind the proficiency to meet predefined performance requirements.

Finally, the flight test data is investigated, by first visualising the flight path of the conducted test flight. Then, the program used for the computation of the position solution, PEGASUS, is discussed, followed by an analysis of the accuracy of standalone signals on the position solution of a GBAS reference receiver antenna. The flight paths based on standalone and GBAS-corrected position solutions are compared and the Protection Levels, which define the integrity of GBAS, are discussed. Furthermore, the reason for peaks in the Protection Levels are explained by taking a look at the used satellite geometry during those peaks. Finally, the Protection Levels are compared with the Alert Limits and the difference of standalone relative to GBAS-corrected position solution is analysed.

Table of Contents

I. List of Figures

II. List of Tables

III. List of Symbols

Symbol	Unit	Description
$1_{(n)}$	m	Estimated line of sight from the position of the user to a satellite as a vector
λ	m	Wavelength of the carrier phase
τ	s	Filter time constant
ρ_k	m	Current raw pseudorange measurement
"^"		This represents the smoothing of pseudorange values
$\hat{\rho}_{air,corr,t}(n)$	m	Corrected smoothed pseudorange at the aircraft receiver
$\hat{\rho}_{air,t}(n)$	m	Measured smoothed pseudorange at an epoch time t
$\hat{\rho}_i(m.n)$	m	Smoothed pseudorange from the receiver m to the satellite n
$\hat{\rho}_k$	m	Current carrier-smoothed pseudorange
$\hat{\rho}_{k-1}$	m	Previous carrier-smoothed pseudorange
$\hat{\rho}$	m	Smoothed Pseudorange
$\Delta\rho(n)$	m	Residuals between the measured and the calculated ranges
ε_p		Noise of code measurement
ε_ϕ		Noise of carrier phase measurement
η_p		Time-varying hardware bias (Code measurement)
η_ϕ		Time-varying hardware bias (Carrier phase measurement)
σ^2		Variance of the differential corrected pseudorange measurement
ϕ_k	m	Current carrier phase measurement input
ϕ_{k-1}	m	Previous carrier-phase measurement input
$\lvert B_{k,apr,lat} \rvert$		Projection of the B-values onto the lateral component
$\lvert B_{k,apr,vert} \rvert$		Projection of the B-values onto the vertical component
b_u	s	User clock offset
e		Ephemeris error
f	Hz	Frequency of the signal
G		Geometry matrix
H_1		Single fault case in the ground system for protection level
H_{eph}		Ephemeris protection level
H_o		Fault-free case for protection level
HAL	m	Horizontal Alert Limit
HPL	m	Horizontal Protection Level
I	m	Ionospheric delay

k_{ffmd}		Fault free missed detection multiplier
k_{md}		Missed detection multiplier
MP_{ρ}		Code multipath
$MP_{\phi,i}$		Phase multipath
$N_i\lambda_i$		Integer ambiguity for the incoming carrier wavelength λ on frequency i
PRC_{CSC}	m	Pseudorange correction candidate
$RRC_{TX,t}$	m	Range rate correction from the related message
r	m	Geometric range
S		Weighted least-squares projection matrix
$s_{apr,lat}$		Projection onto the lateral component
$s_{apr,vert}$		Projection onto the vertical component
S_{EL}	m	Electromagnetic range between the satellite and the receiver
$s_{k,i}$		Entries of the S-Matrix of row k and column j
$s_{vert,i}$		Scalar parameter describing the weight which is given to the measurement of satellite I (vertical)
$s_{lat,i}$		Scalar parameter describing the weight which is given to the measurement of satellite I (lateral)
t_{zcount}	s	Time at which the correction was calculated
Δt_{SV}	s	Satellite clock offset
T	m	Tropospheric delay
TEC	$10^{16}\mathrm{el/m^2}$	Electron density along the signal path
TTA	s	Time to Alert
$v_u^{(k)}$		Measurement errors that occur between user u and satellite k
VAL	m	Vertical Alert Limit
VPL	m	Vertical Protection Level
w_j		Weighting of the respective satellite j
W		Weighting Matrix
$\vec{x}$		x-coordinate of the user position in the ECEF (Earth-Centered-Earth-Fixed) reference (index specifies to which object position appears)

IV. List of Acronyms

AGL ..... *Above Ground Level*
AL ..... *Alert Limit*
ARNS ..... *Aviation Radio Navigation Service*
DH ..... *Decision Height*
DOP ..... *Dilution of Precision*
ESA ..... *European Space Agency*
FMS ..... *Flight Management System*
GBAS ..... *Ground Based Augmentation System*
GLONASS ..... *Globalnaja nawigazionnaja sputnikowaja sistema*
GLS ..... *GBAS Landing System*
GNSS ..... *Global Navigation Satellite System*
GPA ..... *Glide Path Angle*
GS ..... *Glideslope*
HAL ..... *Horizontal Alert Limit*
HPL ..... *Horizontal Protection Level*
LOC ..... *Localizer*
MEO ..... *Medium Earth Orbit*
NSE ..... *Navigation System Error*
Pegasus ..... *Prototype EGNOS GBAS Analysis System Using SAPHIRE*
PL ..... *Protection Levels*
PRN ..... *Pseudo-Random Noise*
RINEX ..... *Receiver Independent Exchange Format*
RNP ..... *Required Navigation Performance*
RNSS ..... *Radio Navigation Satelllite Systeme*
RVR ..... *Runway Visual Range*
SAR ..... *Search and Rescue*
SCA ..... *Smooth Clock Adjust*
SIS ..... *Signal in Space*
TEC ..... *Total Electron Content*
TTA ..... *Time to Alert*
UHF ..... *Ultra High Frequency*
VAL ..... *Vertical Alert Limit*
VDB ..... *VHF Data Broadcast*
VHF ..... *Very High Frequency*
VPL ..... *Vertical Protection Level*

1 Introduction

Over the last century, air transport of passengers and cargo has seen an increase of movements, with forecasts expecting an average growth of 4.3 % per annum over the next 20 years [1]. Growth in air traffic movements results in intermediate congestions of already busy air traffic control sectors over regions such as central Europe. This development leads to a challenging environment in terms of airspace and airport capacity. Furthermore, during low visibility operations, spacing between arriving aircraft and aircraft operating on ground must be increased, which leads to an additional restriction of capacity around airports. Development programs such as Europe's SESAR or the United States' NextGen design Air Traffic Management (ATM) solutions to ensure continuous and safe operations in such conditions. One aspect that is proposed is the increasing use of GNSS, such as the United States' Global Positioning Service (GPS) constellation, as primary means of navigation. With the use of GNSS, navigation performance in terms of accuracy and integrity can be significantly increased compared to conventional navigation aids mostly used today. The navigation performance requirements differ depending on the phase of flight, with the strictest being for the guidance of aircraft on precision approaches and automatic landings. Currently, for these phases of flight, aircraft are mostly guided by the Instrument Landing System (ILS). However, the ILS can only provide straight-in guidance and requires operational mitigation of signal distortions by significant spacing of the aircraft aligned on the approach. Also, it can only provide approaches at one predefined glide slope angle to one fixed aiming point on the runway. One GNSS dependent alternative to the ILS is the Ground Based Augmentation System (GBAS), which is currently certified for commercial operations during CAT-I precision approaches. It is developed to also support commercial CAT-II and CAT-III operations in the near future and is expected to be the replacement for the ILS, which has been the standard for commercial landing systems since 1946 [2], [3]. It uses the standalone GNSS signals and corrects errors induced e.g., by atmospheric propagation or multipath effects by differentially correcting the signals with a reference ground station and antennas in a known location. GBAS is currently only used for straight-in approach guidance similar to the one that ILS supports, but extensive standardization effort is ongoing in order to use the advantages to the fullest extent in the near future. Those advantages include increased and variable glide slope angles for noise abatement, multiple glide slope angles for wake vortex mitigation and therefore less spacing of aircraft on the approach, multiple runway aiming points to optimize separation and minimize runway occupancy and taxi times to ultimately increase the capacity of a runway and vertical guidance of curved approaches. The ultimate goal being the support of automated taxi operations and precision departure guidance. These variable operations are possible due to the flexibility to define reference paths for aircraft by waypoints, straight and curved segments and vertical profiles, whereas the ILS is only capable of uniform straight-in approaches due to its physical limitation. Another benefit is the reduced cost of GBAS compared to the ILS, since it requires only one ground station per airport for operations at every runway from both directions, whereas the ILS requires four ground stations for a single runway in order to allow operations from both directions. Although a GBAS ground station is significantly more expensive than the ILS infrastructure, the reduced cost of maintenance and non-coercion of calibration flights makes GBAS more economically attractive in the long term compared to the ILS.

1.1 Situation at Zurich Airport (LSZH)

On the 10th of March 2011, the first GBAS station in Switzerland was implemented at Zurich Airport (LSZH), thus making a step towards the modernization of its infrastructure and technology [4]. Nevertheless, in 2019, only about three approaches into LSZH per day were performed using GBAS [5]. This is due to the fact that for some, mostly older aircraft, the equipage of a GBAS antenna is either optional or not supported. Swiss International Airlines, the home carrier of LSZH, currently only have two aircraft equipped with a GBAS subsystem, despite the relatively small average fleet age. Also, currently GBAS only supports ILS-lookalike CAT-I operations on runway 14, whereas the ILS supports operations up to CAT-III on runway 14 and 16. Another fact is that pilots tend to rather rely on familiar guidance systems such as the ILS, since it does the job and GBAS cannot provide any significant advantages yet. Thus, with the further development of GBAS, it is anticipated to someday replace the ILS stations at LSZH, providing more flexible operations, reducing congestion-related delays and ultimately increase the airports capacity.

1.2 Objectives of this Work

The general objective of this work is to evaluate the commercially operational GBAS performance in flight trials at LSZH by comparing the GBAS-corrected experimental flight test data with its own “raw” standalone position solution. The recorded GBAS corrections and the standalone GPS data are investigated with the use of the PEGASUS Tool by EUROCONTROL. The goal is to gain a general idea of the correction process done by GBAS and to find trends for any anomalies found in the evaluated data.

The data to be evaluated was gathered on the 10th of September 2019 with an Airbus A320 by the DLR. The aircraft was based in Dübendorf Air Base (LSMD) during the flight trials. Due to the scope of this work, only around a one-hour period of the flight test data is investigated.

This work is neither considering any comparison of GBAS and ILS operations, nor the performance of satellite-based departures. It is solely assessing the GBAS’ operational capability to correct standalone GNSS signals for CAT-I precision approaches with the PEGASUS program.

2 Background

In the last century, air travel has seen a growth in aircraft movements that forced large airports to operate at their maximum capacity, especially in conditions with low visibility or sudden changes of weather or wind. To ensure safe runway approaches in such conditions, landing aids are developed that provide vertical and horizontal guidance to the pilots. Nowadays, nearly every commercial airport allows operations with such a landing aid, the most common being the ILS, which is explained in the following Chapter, Instrument Landing System (ILS). The continuous development of technology in the aviation industry leads to the introduction of more cost efficient, flexible and GNSS-based landing aids such as the GBAS, which will be explained in Chapter 4, Ground Based Augmentation System (GBAS).

2.1 Instrument Landing System (ILS)

The ILS is an aid used for precision runway approaches, providing vertical and horizontal guidance for pilots as well as autopilots with the use two radio beams with different frequency each for the horizontal and the vertical plane (see Figure 1). The localizer (LOC) provides azimuth guidance, whereas the glideslope (GS) provides a continuous vertical descent profile reference. The LOC transmits two narrow intersecting beams, one slightly to the left modulated with a 150 Hz signal and one slightly to the right of the centreline modulated with a 90 Hz signal. The intersection of those two beams is the ideal runway centreline extension, which is detected by airborne equipment to provide pilots information about the horizontal displacement. The LOC aerials are located behind the end of the runway. The GS similarly transmits two beams to provide vertical guidance reference so that the intersection of the four beams defines an approach guidance in the three-dimensional space. The GS aerials are usually located so that the arriving aircraft crosses the runway threshold typically at 50 ft above ground level (AGL), with a GS angle of typically three degrees. Variations may occur for some runways due to terrain or noise abatement in the approach sector or other necessities. An approach shall not be continued unless the runway visual range (RVR) and the minimum at the decision height (DH) are met, which both depend on the ILS category of a certain approach, otherwise, a go-around shall be flown. ICAO Annex 6, Operation of Aircraft defines the RVR as *"the range over which the pilot of an aircraft on the centre line of a runway can see the runway surface markings or the lights delineating the runway or identifying its centre line",* and the DH as *" a specified altitude or height in the Precision Approach or approach with vertical guidance at which a Missed Approach must be initiated if the required visual reference to continue the approach has not been established" [7].* Different ILS categories are defined depending on the crew qualification, aircraft equipment and runway configuration (see Table 1) [8].

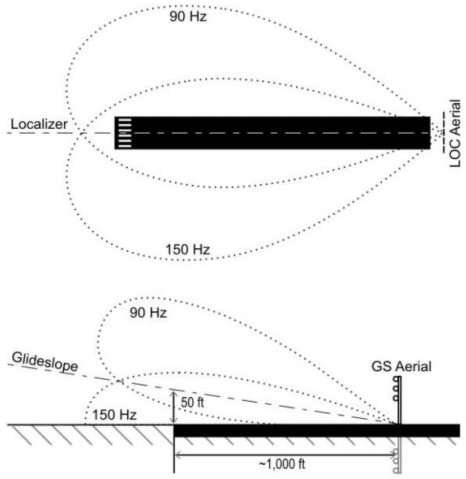

Figure 1, LOC and GS radio beams used for ILS precision approach guidance [6].

Category of Operation	Decision Height (DH)	Runway Visual Range (RVR)
CAT I	DH ≥ 200 ft (60m)	RVR ≥ 1800 ft or visibility ≥ 2600 ft
CAT II	100 ft ≤ DH < 200 ft	RVR ≥ 1000 ft
CAT III A	No DH or DH < 100 ft	RVR ≥ 550 ft
CAT III B	No DH or DH < 50 ft	160 ft ≤ RVR < 550 ft
CAT III C	No DH	No RVR limitation

Table 1, ILS Categories and their respective values for Decision Height and Runway Visual Range. It is important to note that ILS CAT IIIC is currently not in use [7].

2.1.1 Limitation of the ILS

In today's civil aviation, the ILS is almost always used for approach guidance. In its history of almost 90 years, it helped pilots all over the world land their aircraft in low visibility and brought standardization to airports approach sector due to its consistent and uniform approach guidance. Nevertheless, the ILS as it is used today also brings its downsides, especially at congested airspace systems, where the arrival rate is high. One potential hazard to this system is the location of the LOC aerials. Its position at the end of the runway makes the transmitted signal vulnerable to reflections or distortions by preceding aircraft, as well as obstacles near the runway or the surrounding terrain. The departing aircrafts fuselage, wings and horizontal stabilizer can generate shading and multipath effects, which ultimately lead to incorrect horizontal guidance for the approaching aircraft. Similar disturbances can occur with departing aircraft holding short of runways, blocking the GS signal transmitted by the GS aerial. Thus, during low visibility conditions, spacing between departing and arriving aircraft as well as between consecutive arrivals must be increased and areas in the vicinity of the runway must be kept clear of traffic. These measures lead to a decrease in the airport's capacity, often resulting in flight delays and cancellations. The ILS can be adapted to certain runway and approach sector requirements such as noise abatement or terrain. This is achieved by using higher glide slopes angles in the beginning of the approach, displaced thresholds or curved approach segments. Nevertheless, it eventually only provides straight-in final approach guidance. These restricting measures can be rectified with the implementation of a GBAS Landing System, which is described in Chapter 4, Ground Based Augmentation System (GBAS) [9].

2.2 Global Navigation Satellite System (GNSS)

Originally designed for warship navigation by the US and USSR military, Global Navigation Satellite Systems (GNSS) are nowadays widely used in the civilian area. Consisting of different satellite constellations, GNSS provide precise navigation based on the principle of multilateration. An object's position is accurately defined by its latitude, longitude, and height above ellipsoid of the earth. By knowing the instantaneous position of three satellites and their distances to the object, the location of the object can be determined in all three dimensions. To synchronize the satellite clock and the user clock, a fourth satellite is used as a reference. An extensive explanation on the operating principle is to be found in Chapter 2.2.2, Operating Principle.

2.2.1 Core Constellations

This chapter is according to [10]. The oldest system providing GNSS service is the US GPS that began operations in 1978, currently operating 32 satellites in Medium Earth Orbit (MEO). Its orbits are designed to make at least six satellites visible at any time at all locations on earth, to ensure a continuous, reliable service, providing accuracy of 10 m for public and 5 m for military use.

The Globalnaja nawigazionnaja sputnikowaja sistema (GLONASS) is the Russian equivalent to GPS that became operational in 1993. Global coverage was achieved in 2015 by 23 operating satellites in MEO with a similar accuracy than GPS. By a combination of GPS and GLONASS, receivers have access to over 50 satellites, thus ensuring a quicker position determination, especially in urban canyons or remote mountain areas.

China's BeiDou-2 is a system planned to consist of five geostationary, five inclined geosynchronous and 25 medium earth orbit satellites, thus generating global coverage as well as a more thorough service to China and its neighbourhood. It is expected to become fully operational by late 2020, providing an accuracy of 10 m for public and higher for military use.

GALILEO is a satellite constellation owned by the European Commission and operated by the European Space Agency (ESA). Its main difference to GPS and GLONASS is its independent civilian use, while GPS, GLONASS and BeiDou are controlled and operated by the military. GALILEO's service is planned to be more precise than other constellations, providing an accuracy of one meter for public use and up to centimetre-accuracy for paid users. GALILEO will nominally consist of 30 satellites, of which 22 are currently in orbit. Although, currently two of those are damaged and therefore not operational.

2.2.2 Operating Principle

In order to determine a user's location on earth, one navigation equation for each of the four satellites necessary for multilateration is used. This navigation equation in its most simplified version is given in Equation (1), where $\tau^{(k)}$ represents the range from the user to the satellite k.

$$\tau^{(k)} = \sqrt{(x_u - x^{(k)})^2 + (y_u - y^{(k)})^2 + (z_u - z^{(k)})^2} + b_u + v_u^{(k)} \quad (1)$$

In this equation, x_u, y_u, and z_u represent the location of the user in a XYZ coordinate-system, whereas $x^{(k)}$, $y^{(k)}$ and $z^{(k)}$ represent the location of the satellite k in the same coordinate system. b_u stands for the user clock offset relative to the satellite time and $v_u^{(k)}$ stands for all the other measurement errors that occur between user u and satellite k, which will be elaborated more in Equation (2).
The navigation equation contains the estemandas, which means "quantity to be estimated". Those are the parameters that need to be solved for in order to determine the location of the user. The estemandas in this case are x_u, y_u, z_u and b_u. The variables $x^{(k)}$, $y^{(k)}$ and $z^{(k)}$ are known since they can be calculated from the orbit

parameters. These orbit parameters are contained in the navigation message. The user clock offset b_u is the same in all pseudorange measurement equations and therefore it is possible estimate it.

The term

$$\sqrt{(x_u - x^{(k)})^2 + (y_u - y^{(k)})^2 + (z_u - z^{(k)})^2}$$

corresponds to the mathematical 2-norm and is therefore nothing else than the Euclidean distance, or rather the geometric range r between the user and the satellite. Through the application of a Taylor-Series, the navigation equation can be linearized, allowing a simpler solving of the equation.

In addition to the navigation code-based pseudorange measurements, the carrier phase of the signals is measured and available as observables at the output of the receiver. Although these measurements are very precise, the number of cycles between the satellite and the receiver is not known and therefore making them equivocal. The code and carrier phase measurement by the true range and including the associated errors are described as

$$\begin{aligned} \rho_i &= r + b_u + T + I_i + e + MP_{\rho,i} + \varepsilon_{p,i} + \eta_{p,i} \\ \phi_i &= r + b_u + T - I_i + e + N_i\lambda_i + MP_{\phi,i} + \varepsilon_{\phi,i} + \eta_{\phi,i} \end{aligned} \tag{2}$$

Where r is the geometric range from the user to the satellite, b_u is the user clock offset relative to the satellite time, T is the tropospheric delay, I_i is the ionospheric delay for frequency i, e is the ephemeris error, $MP_{\rho,i}$ and $\varepsilon_{p,i}$ are the code multipath and noise on frequency i, $MP_{\phi,i}$ and $\varepsilon_{\phi,i}$ are the phase multipath and noise on frequency i, $N_i\lambda_i$ describes the integer ambiguity for the incoming carrier wavelength λ on frequency i, and $\eta_{p,i}$ and $\eta_{\phi,i}$ represent the time-varying hardware bias introduced on the code, which can be for example due to the antenna or receiver.

The rate of change of the carrier phase measurements can be used to perform a carrier-smoothing, where the high frequency noise and multipath from the code measurements can be reduced [11]. The noisy, but unambiguous code pseudorange measurement can be smoothed with the precise, but ambiguous carrier-phase measurements. This carrier-smoothed code measurement is achieved by adding the measurement between two epochs to the previous smoothed pseudorange measurement. These changes in phase measurement can provide an estimate of the change in receiver position over time and in the direction of the satellite generating the phase [12].
The equation for the smoothed pseudorange is described as

$$\hat{\rho}_k = \frac{\Delta t}{\tau}\,\rho_k + \left(1 - \frac{\Delta t}{\tau}\right)(\hat{\rho}_{k-1} + \lambda(\phi_k - \phi_{k-1})) \tag{3}$$

Where $\hat{\rho}_k$ is the current carrier-smoothed pseudorange, $\hat{\rho}_{k-1}$ is the previous carrier-smoothed pseudorange, ρ_k is the current raw pseudorange measurement, ϕ_k is the current carrier phase measurement input, ϕ_{k-1} is the previous carrier-phase measurement, λ is the wavelength of the carrier phase, Δt is the sample interval and

τ is the filter time constant. This Equation (3) is then implemented into the raw pseudorange Equation (2), generating a final equation of the smoothed pseudorange that is formulated as

$$\hat{\rho}_i = r + b_u + \hat{T} + \hat{I}_i + \hat{e} + \widehat{MP}_{\rho,i} + \hat{\varepsilon}_{p,i} + \hat{\eta}_{p,i} \quad (4)$$

where the operator hat "ˆ"represents the corresponding symbols after smoothing. This final smoothed pseudorange $\hat{\rho}$ is an accurate enough measurement to determine the range between the satellite and the receiver. Although multipath and noise error can be minimized, smoothing introduces additional delay through time variant error sources such as the ionosphere or code hardware biases. Due to the fact that there ultimately are four pseudorange equations (one per satellite), and a minimum of four unknowns, the satellite navigation is a 4-dimensional system with time as the fourth dimension.

2.2.3 GNSS Signals

GNSS uses the L-Band which is in the Ultra High Frequency (UHF) part of the frequency spectrum. Satellites continuously transmit navigation signals in two or more frequencies in the L-Band, which ranges from 1 GHz to 2 GHz [13]. These navigation signals contain ranging codes and navigation data that allow users to compute the coordinates of the satellite at any epoch, as well as determine the travel time of the signal from the satellite to the receiver. The main signal components are characterised as follows [14];

The Carrier: Radio frequency sinusoidal signal at a given frequency, onto which the navigation code is modulated with the use of phase modulation.

The Ranging Code: Sequences of 0s and 1s (zeroes and ones), which allow the receiver to determine the travel time of radio signal from satellite to receiver. They are called Pseudo-Random Noise (PRN) sequences or PRN codes.

The Navigation Data: A binary-coded message providing information on the satellite ephemeris (Keplerian elements or satellite position and velocity), clock bias parameters, almanac (with a reduced accuracy ephemeris data set), satellite health status, and other complementary information.

Figure 2 shows the different frequency bands used for the Radio Navigation Satellite System (RNSS) and for the Aviation Radio Navigation Service (ARNS). No other users are allowed to interfere with the signals used for ARNS, making them suitable for critical, safety dependent operations such as Aviation. GPS uses the L5, L2 and L1 bands, whereas GLONASS uses the G3, G2 and G1 bands. Coexisting in the same frequency as GPS's L5 and L1 and GLONASS's G3, GALILEO uses the E5a, E1 and E5b, respectively. The signals in the 1215 MHz to 1300 MHz spectrum are primarily allocated to RNSS and radio-location services such as ground radars, thus making them more vulnerable to interference than the ones used by ARNS. The signals ranging from 1544 MHz to 1545 MHz are used for the GALILEO Search and Rescue

(SAR) operations, which, with the use of three strategically deployed ground stations across Europe, helps to locate and help people in distress.

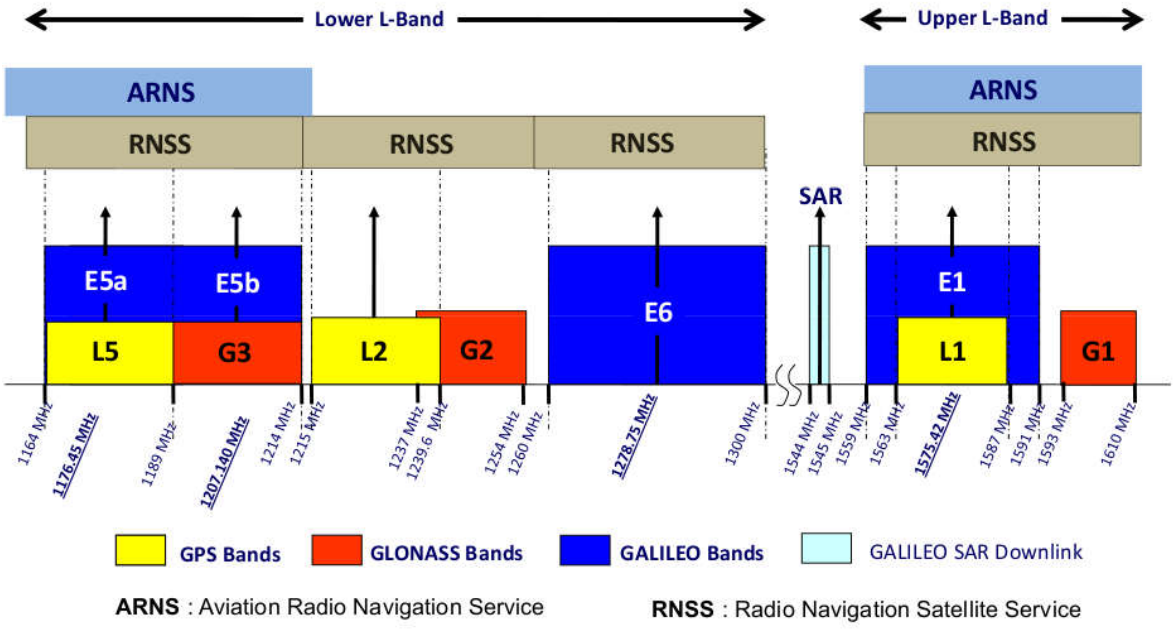

Figure 2, Frequency Spectrum with the different bands used for GNSS [15].

3 GNSS Error Sources

In satellite navigation, there are many different error sources, which strongly differ in their impact on satellite navigation precision and are caused by different sources. These errors can be divided into those originating at the satellite, those originating at the receiver and those that are due to signal propagation by atmospheric refraction. Here only the main error sources that have the biggest influence for aviation users are considered.

3.1 Ionospheric Delay

The ionosphere is an atmospheric layer between around 60 km and 2000 km, which contains a large number of ionized particles. It spreads from the mesosphere over the thermosphere to the exosphere. The ultraviolet and x-ray radiation from the sun interacts with the gas molecules and atoms, which leads to gas ionization. This plasma bends ranging signal by refraction and changes their propagation speed as seen in Figure 3. The range error introduced by the ionosphere is given in Equation (5), where S represents the electromagnetic, rather than the geometric, range between the satellite and the receiver, ρ is the geometric range between the satellite and the receiver, TEC is the integrated electron density along the signal path (Total Electron Content) and f is the frequency of the signal [17].

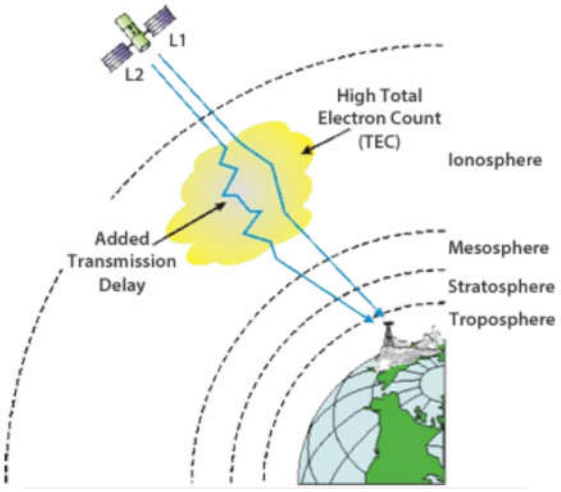

Figure 3, Effects of the Ionosphere on the satellite signal [16].

$$S = \rho + 40.3 \cdot \frac{TEC}{f^2} \tag{5}$$

Through the plus-operator it can be seen that S will always be longer than ρ, thus being a delay due to the signal's longer transmission time. It can also be seen that the ionospheric delay is inversely proportional to the square of the frequency of the signal, which means that the higher the frequency, the lower the ionospheric delay.
Additional to the range error, the ionosphere also causes a curvature of the signal. Although the curvature of the signal path causes an extremely small, almost negligible range error, the change in propagation speed can already cause significant errors.

There are possibilities to minimize the error of the ionosphere by the use of dual frequency techniques. However, this solution is not completely satisfactory, because other errors such as the influence of multipath, are amplified or there is too much dependence on the gradient of the ionosphere, which is the difference between S and ρ, as seen in Equation (5) [18].

Another important point is that the delay of the ionosphere depends on the position of the satellite as seen from the user. If the satellite observed by the user is at the zenith, the signal's path through the ionosphere is shorter than if the satellite is seen at a small elevation angle close to the horizon. This means that the error introduced by the ionosphere for a certain satellite is at its highest when the satellite rises or sets at the horizon as seen from the user and is at its lowest if the satellite is at its zenith relative to the user.

3.2 Tropospheric Delay

Another atmospheric perturbation is the delay introduced by the troposphere. Although, the variability of the tropospheric impact is much smaller compared to that of the ionosphere. The troposphere is the lowest layer of the atmosphere and goes up from the earth's surface to about 50 km. It consists of dry gas and water vapour and is an electrically neutral layer of the earth's atmosphere, which means it is not ionized. Similar to the ionosphere, the troposphere also extends the time of the signal by refraction and its impact on the satellite signal error depends on the elevation angle of the satellite relative to the user. The total delay can be divided into the wet and the dry component. The dry component, which makes about 90 % of the total error, is a function of pressure and temperature, whereas the wet component is a function of the humidity. The dry component is easier to determine than the wet component, which is due to the difficulties in predicting water vapour distribution from surface measurements.

The effect on the satellite signal through the troposphere is different compared to the ionosphere. The troposphere is refracting, where the refraction of the signal is not dependent on the frequency if it is below 30 GHz [17]. Therefore, the known frequency bands of GNSS L1, L2 and L5, are refracted equally. The refraction is equivalent to a delay in the arrival of the signal from a GPS satellite. This means that the range between receiver and satellites appears to be greater than it is due to the signal being delayed and taking more time to reach the receiver.
The tropospheric delay experienced by a user depends on whether a satellite is at the zenith or at the horizon as seen from the user, because the path of the signal through the troposphere is longer when the satellite is at the horizon than when it is at the zenith. Thus, similar to the error introduced by the ionosphere, the quality of positioning with a satellite appearing on the horizon increases until the satellite is at the zenith as seen from the user, and then the accuracy gradually decreases until the satellite disappears behind the horizon.

3.3 Multipath

Multipath, together with the ionospheric error, is one of the main sources of error in GNSS. Multipath occurs when the receiving antenna receipts a signal via multiple paths (a mixture of refracted and direct paths) rather than from a sole direct line of sight, as seen in Figure 4. This results in a distortion of the correlation peak in the receiver when determining the pseudorange. Refraction usually occurs if a signal is deflected by surfaces such as buildings or other aircraft, or really any reflective surface. These do not necessarily have to be large to cause multipath errors. This combination of multiple paths increases the measurement of the propagation time and thus increases the pseudorange measurement, making the range between the satellite and the receiver seem longer than it actually is [19].

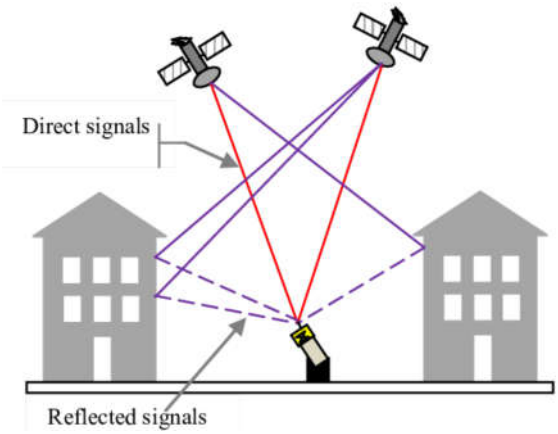

Figure 4, Multipath Effects on the satellite signal [18].

3.4 Orbital Errors

The GNSS receivers calculate the coordinates relative to the known locations of the satellites. The shape of the satellite orbits and their speed is known. Control centres monitor satellite parameters that directly contribute to the satellite position error and then compile these in the so-called ephemeris. These ephemerides are recorded for each satellite and are also broadcasted from each satellite. Due to error budgets regarding the satellite orbit determination and clock accuracy, the ephemerides can contain errors that can result in a position inaccuracy of 2 to 5 m for the user [20].

3.5 Satellite Geometry

The satellite geometry is not an actual error source, although it has a direct bearing on the quality of the position derived from them. The accuracy of the satellite navigation is subject to a geometric phenomenon called Dilution of Precision (DOP). The DOP concerns the geometric strength of the position solution described by the positions of the satellites with respect to one another or to the receivers. The lower the DOP value, the more optimal the satellite configuration and therefore the higher the quality of the position derived from them, as seen in Figure 5.

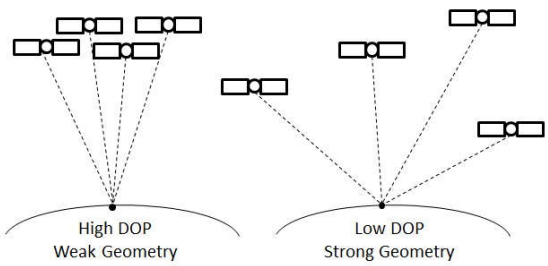

Figure 5, Weak and Strong Satellite Geometries with High and Low DOP, respectively [21].

Additional to the DOP, the number of satellites available also plays a role in the accuracy of satellite navigation. It can be generally said that the more satellites are visible from the user location, the smaller the contribution of each satellite to the

position solution and therefore the smaller the influence of an error generated by a single satellite. The integrity as well as the accuracy can be adversely affected by only using a minimum of four satellites for a position solution, which is why it is optimal to generate a position solution using a larger number of available satellites.

4 Ground Based Augmentation System (GBAS)

A Ground Based Augmentation System (GBAS) provides approach geometry, integrity monitoring and differential corrections of GNSS data transmitted to aircraft with the use of a reference ground station. It is primarily used for GNSS-based precision approaches (GLS), described in Chapter 4.1, Purpose of GBAS Landing System. The goal of a GBAS is to provide signal accuracy, integrity, continuity and availability for aircraft operations [22].

4.1 Purpose of GBAS Landing System (GLS)

A GBAS Landing System (GLS) is a GNSS-dependent alternative to the widely known ILS, which is described in Chapter 2.1, Instrument Landing System (ILS). GLS uses a single GBAS ground station to transmit corrected GNSS data to suitably equipped approaching aircraft, providing an approach guidance reference with greater flexibility compared to ILS. With the use of GLS, non-linear precision approaches and flexible horizontal profiles can be flown, compared to the uniform and linear precision approach guidance transmitted by the ILS. Although, it is important to note that the final approach sector still has to be a straight line due to the limitations by the aircraft. Furthermore, all runways of a GBAS-equipped airport can be supported by a single GBAS ground station, theoretically allowing up to 48 simultaneous precision approaches. This reduces cost of infrastructure and maintenance compared to ILS, which requires four ground stations (two LOC aerials and two GS aerials) per runway in order to allow precision approaches in both directions [23].

4.2 GBAS Infrastructure Subsystems

The GBAS infrastructure as seen in Figure 6 can be divided into three main components:

- The Satellite Subsystem
- The Ground Subsystem
- The Aircraft Subsystem

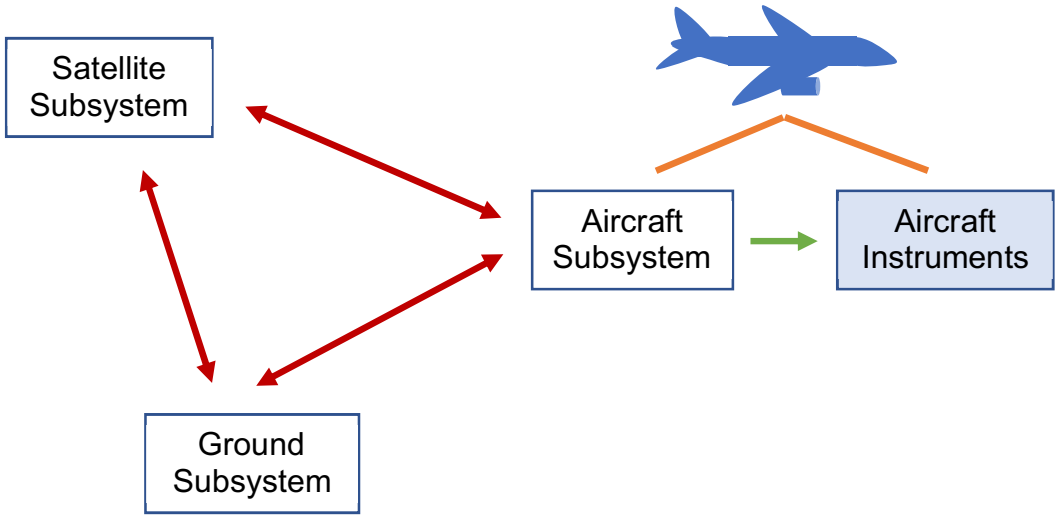

Figure 6, Interconnectedness of the Satellite Subsystem, Ground Subsystem and Aircraft Subsystem.

The satellite subsystem is composed by the GNSS ranging sources and transmits the ranging signals and navigation messages both to the aircraft and to the ground subsystem. These GNSS ranging sources consist of GPS and GLONASS constellations.

4.2.1 Ground Subsystem

A GBAS ground subsystem as seen in Figure 7 normally consists of four GPS antennas, a central processing system (Ground Facility) and a VHF Data Broadcast (VDB) transmitter. These facilities are all located at the airport itself. The ground facility uses a VHF radio link to send data to aircraft that consist of GPS corrections, integrity parameters and approach path information. This radio link operates in the frequency range between 108 MHz and 118 MHz Each reference receiver measures the propagation errors introduced by atmospheric refraction for its receiver location. The average of these measurements is then applied to the satellite ranges measured by the GBAS avionics which are therefore corrected. The ground facility is also used to monitor general GPS satellite performance such as the satellites health. If a satellite sends incorrect data, the ground facility stops broadcasting from the affected satellite and corrects it with the use of another satellite in order to prevent the transmission of incorrect data to the GBAS avionics on board the aircraft (see Chapter 4.3.2, Integrity). Confidence that the aircraft's calculated and differentially corrected position is accurate is achieved through additional parameters sent by the ground facility. Those parameters are used by the GBAS avionics to determine error bounds on the calculated GPS position. Furthermore, an updated correction message is broadcasted twice a second through the VDB transmitter. These messages contain the corrections and less frequently, integrity parameters, ground facility characteristics and approach path guidance. The VDB broadcasts the signal throughout the GBAS coverage area to the GBAS avionics of the aircraft subsystem. The GBAS provides its service to a local area in which continuous support of the aircraft is provided, from the en-route airspace through the terminal airspace to the precision approach and landing in a radius of about 42 km [24] around the ground station [25].

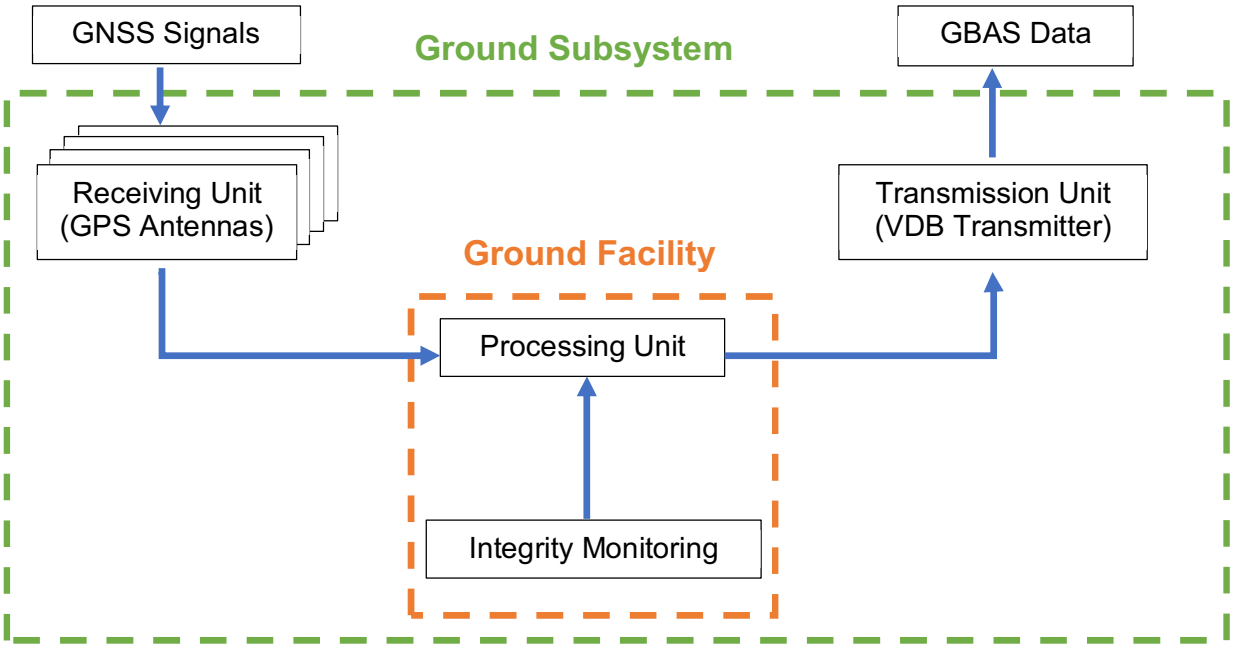

Figure 7, The Ground Subsystem with its Ground Facility, which generates the GBAS corrections.

4.2.1.1 Ground Subsystem Correction Generation

With a measurement from a reference receiver, the ground subsystem can calculate a carrier-smoothed pseudorange correction for the satellites in view. The position of the reference antenna is precisely known, which has the advantage that the position of the satellite can be calculated by the use of the navigation message. Therefore, the geometrical range to each satellite in view can be determined.

By subtracting the smoothed pseudorange and the satellite clock bias from the geometric range, a pseudorange correction PRC_{CSC} can be calculated for each candidate:

$$PRC_{CSC}(m,n) = r(m,n) - \hat{\rho}_i(m.n) - c \cdot \Delta t_{SV}(m,n) \quad (6)$$

Where r describes the geometric range from the receiver m to the satellite n, $\hat{\rho}_i(m.n)$ is the smoothed pseudorange, $\Delta t_{SV}(m,n)$ is the clock bias calculated for the satellite n, based on the navigation message received from a user m. The i always describes the frequency in the context.
With the carrier smoothed pseudorange from Equation (3) the PRC_{CSC} can be written as:

$$PRC_{CSC}(m,n) = -c \cdot \Delta t_m - \hat{T} - \hat{I}_i - \widehat{MP}_{\rho,i} - \hat{\varepsilon}_{\rho,i} - \hat{\eta}_{\rho,i} \quad (7)$$

The PRC_{CSC} contains the receiver clock offset, which can be removed by the so-called smooth clock adjust (SCA). The smooth clock adjust removes a weighted average of all pseudorange corrections for a given receiver.

$$PRC_{SCA}(m,n) = PRC_{CSC}(m,n) - \sum_{j=1}^{N} w_j \, PRC_{CSC}(m,j) \tag{8}$$

The formula gives the correction for a receiver m and a satellite n after the smoothed clock adjust, where N is the number of satellites involved and w_j is the weighting of the respective satellite.

With the pseudorange correction, it is possible to calculate a broadcast correction for a satellite n. This broadcast correction is calculated from the average of all pseudorange correction candidates for one satellite over all receivers.

$$PRC_{TX}(n) = \frac{1}{M} \sum_{k=1}^{M} PRC_{SCA}(k,n) \tag{9}$$

To the pseudorange corrections, additional range rate corrections $RRCs$ are broadcasted from the ground. These are calculated as the rate of change of the current and previous transmitted $PRCs$:

$$RRC_{TX,t}(n) = \frac{PRC_{TX,t}(n) - PRC_{TX,t-1}(n)}{\Delta t} \tag{10}$$

4.2.2 Aircraft Subsystem

A GBAS aircraft subsystem as seen in Figure 8 normally consists of a GPS antenna, a VHF Data Broadcast (VDB) antenna as well as associated processing equipment. GBAS avionics are standard on all new Boeing aircraft that are delivered these days, and optional on the Airbus A320, A330, A350 and A380. Either the pilot selects a predefined approach from the Flight Management System (FMS), or he enters a five-digit channel number through the pilot's interface in order to access the broadcasted data. The VDB antenna receives the corrections sent by the ground subsystem, namely the VDB transmitter. These corrections are then applied to the pseudorange measurements taken by the GNSS receiver on board the aircraft. Then they are computed through the processing equipment (Processor) in order to gain more accurate GPS position, velocity and time to guide the aircraft safely to the runway. The signal provides guidance, which is similar to the ILS, thus making minimal difference to the aircraft instruments such as the primary flight display or the flight control system [20].

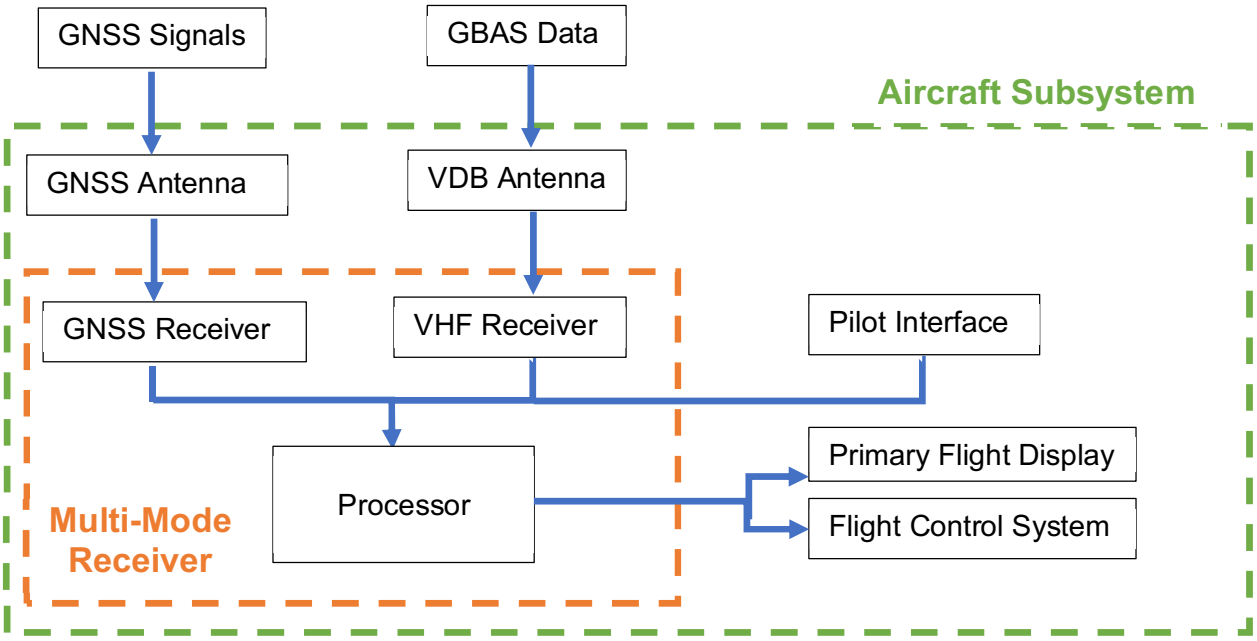

Figure 8, The Aircraft Subsystem with its Multi-Mode Receiver, which applies the GBAS corrections to the GNSS signals.

4.2.2.1 Aircraft Subsystem Correction Generation

This chapter is according to [26]. The aircraft receives the smoothed pseudorange and range rate corrections and uses them to correct its own smoothed pseudorange measurement. The corrected smoothed pseudorange at the aircraft receiver is given as

$$\hat{\rho}_{air,corr,t}(n) = \hat{\rho}_{air,t}(n) + PRC_{TX}(n) + RRC_{TX}(n) \cdot (t - t_{zcount}) + TC + c \cdot \Delta t_{SV} \quad (11)$$

Where $\hat{\rho}_{air,t}(n)$ is the measured smoothed pseudorange at an epoch time t, $PRC_{TX}(n)$ is the broadcast correction from the ground subsystem, $RRC_{TX}(n)$ is the range rate correction from the related message, TC is the differential tropospheric correction, Δt_{SV} is the satellite clock offset and t_{zcount} describes the time at which the correction was calculated.

By using the pseudorange measurement $\hat{\rho}_{air,t}(n)$ and the corrections broadcast by the ground subsystem it is possible for the user to calculate the position coordinates x(x_u, y_u, z_u) and the clock error $c \cdot \Delta t_u$ by

$$\hat{\rho}_{air,corr,t}(n) = \|x(n) - x\| + c \cdot \Delta t_u + \tilde{\varepsilon}_\rho(n) \quad (12)$$

A further position x_0 is given by

$$\hat{\rho}_0(n) = \|x(n) - x_0\| + c \cdot \Delta t_u + \tilde{\varepsilon}_\rho(n) \quad (13)$$

This equation calculates an estimated position, which is made by the last known position.

In a next step the residuals $\Delta\rho(n)$ between the measured and the calculated ranges are calculated by linearization using the Taylor series.

$$\Delta\rho(n) = \hat{\rho}_{air,corr,t}(n) - \hat{\rho}_0(n) = -1_{(n)}\Delta x + \Delta b + \tilde{\varepsilon}_\rho(n) \tag{14}$$

where $1_{(n)}$ is the estimated line of sight from the position of the user to a satellite as a vector.

If the sight line vector is inserted into the geometry matrix, Equation (14) can be written as:

$$\Delta\rho = G\begin{bmatrix}\Delta x \\ \Delta b\end{bmatrix} + \tilde{\varepsilon}_\rho \tag{15}$$

This equation can be solved iteratively. The solution is done by moving the linearization point according to the least-squares solutions for the estemandas. When measuring the satellite broadcast, different levels of noise can occur. These noise intensities depend on factors such as the elevation angle of the satellite relative to the user. An additional weighting is introduced, which gives more weight to satellites where fewer measurement errors are expected. The estemandas are then calculated using a least square approach.

$$\begin{bmatrix}\Delta x \\ \Delta b\end{bmatrix} = (G^T W G)^{-1} G^T W \Delta\rho = S\Delta\rho \tag{16}$$
$$S = (G^T W G)^{-1} G^T W$$

In Equation (16), S describes the weighted least-squares projection matrix. The projection factors relating the GNSS measurements from satellite i to the position domain in approach coordinates play an important role in the integrity assurance process, and the contribution of a single satellite i to the position estimate vertical to the approach track is given by

$$s_{vert,i} = s_{3,i} + s_{1,i} \cdot \tan(GPA) \tag{17}$$
$$s_{lat,i} = s_{2,n}$$

Where $s_{vert,i}$ and $s_{lat,i}$ are vertical and horizontal scalar parameters describing the weight, which is given to the measurement of satellite i, $s_{k,i}$ are the entries of the S-Matrix of row k and column i and GPA is the glide path angle of the approach. Depending on the set of satellites used for GBAS corrections, $s_{vert,i}$ is nominally limited to values smaller than 4. As seen in Chapter 3.5, Satellite Geometry, it can be generally assumed that the more satellites are available for GBAS corrections, the lower the s_{vert} value and therefore the lower the impact of a pseudorange measurement error by a single satellite i on the position solution.

The weighting matrix W is the inverse of the covariance matrix of the measurements and is described as

$$W = \begin{bmatrix} \sigma_1^2 & 0 & 0 & 0 \\ 0 & \sigma_2^2 & 0 & 0 \\ \dots & \dots & \dots & \dots \\ 0 & 0 & 0 & \sigma_n^2 \end{bmatrix} \quad (18)$$

The weighting matrix contains the differences of the variances of the measurement errors from the different satellites and σ^2 is the variance of the differential corrected pseudorange measurements.

4.3 GBAS Performance Characteristics

In order to provide Signal in Space (SIS) for safe and reliable GNSS operations, four parameters are used: Accuracy, Integrity, Continuity and Availability. Those parameters are defined by ICAO and specify the Required Navigation Performance (RNP) for GNSS operations that have to be met for each phase of the flight. For the GBAS operations, the RNP characterizes both the sole performance of a navigation system and the joint performance of the navigation and flight control systems. Compared to GBAS's four RNP parameters, accuracy is the only of the four parameters that is required to be met for standalone GPS [27]. A complete table of the GNSS SIS requirements is given in Table [28].

Typical Operations	**Horizontal Accuracy 95 %**	**Vertical Accuracy 95 %**	**Integrity**	**Time to Alert**	**Continuity**	**Availability**
En-route	3.7 km	N/A	$1-10^{-7}$/ h	5 min	$1-10^{-4}$ / h to $1-10^{-8}$ / h	0.99 to 0.99999
En-route, Terminal	0.74 km	N/A	$1-10^{-7}$/ h	15 s		
Initial Approach, Intermediate Approach, Non-Precision Approach and Departure	220m	N/A	$1-10^{-7}$/ h	10 s		
Approach operation with vertical guidance (APV-I)	220 m	20 m	$1-2*10^{-7}$ per approach	10 s	$1-8*10^{-6}$ per 15 s	
Approach operation with vertical guidance (APV-II)	16 m	8 m	$1-2*10^{-7}$ per approach	6 s		
Category I Precision Approach (CAT-I)	16 m	6 to 4 m	$1-2*10^{-7}$ per approach	6 s		

Table 2, GNSS SIS performance requirements [28].

4.3.1 Accuracy

Accuracy is measured by the GNSS position error which, according to ICAO, "*is the difference between the estimated position and the actual position. For an estimated position at a specific location, the probability should be at least 95 per cent that the position error is within the accuracy requirement." (ICAO Annex 10) [29].*

The accuracy is subdivided into the horizontal and the vertical accuracy, which define the permitted lateral and altitude dependent deviation for different operations, which have to be met during at least 95 % of the operations. An error in the estimation of an aircraft's position is referred to as Navigation System Error (NSE), which defines the GNSS position error. GPS and GLONASS have the capability to provide accurate position and time information worldwide. The accuracy achieved by these constellations is sufficient to meet aviation requirements for en-route through non-precision approach, but not for precision approaches (see Table 3). This lack of accuracy for precision approaches is solved with the use of differential corrections by an augmentation system such as GBAS [30].

	GPS global average 95 % of the time	GLONASS global average 95 % of the time	**CAT-I Precision Approach requirements for 95 % of the time**
Horizontal Position Error	13 m	19 m	**16 m**
Vertical Position Error	22 m	29 m	**4 to 6 m**

Table 3, GPS and GLONASS Position accuracy and CAT-I Precision Approach requirements [29].

4.3.2 Integrity

For safety of life applications, such as navigation for automatic landings, not only accuracy is important, but especially the integrity.

ICAO defines integrity as "*A measure of the trust that can be placed in the correctness of the information supplied by the total system. Includes the ability of a system to provide timely and valid warnings to the user (alerts)." (ICAO Annex 10) [29]*

For GBAS operations, integrity is assured by the introduction of Protection Levels (PL). These PLs are subdivided into the Horizontal Protection Level (HPL) and the Vertical Protection Level (VPL). These values are conservative bounds of the actual positioning error that can be calculated based on standardized models for different error contributions. Three PLs are calculated: one for the fault-free case (H_o), one for a single fault case in the ground system (H_1) and an ephemeris protection level (H_{eph}), which will not be discussed further in the scope of this work.

The fault-free protection levels H_0 are influenced by the nominal measurement error models and the satellite geometry. They are defined as

$$VPL_{H_0} = k_{ffmd}\sqrt{\sum_1^N s_{apr,vert,n}^2 \cdot \sigma_n^2} \tag{19}$$

$$HPL_{H_0} = k_{ffmd}\sqrt{\sum_1^N s_{apr,lat,n}^2 \cdot \sigma_n^2} \tag{20}$$

Where k_{ffmd} represents the fault free missed detection multiplier, $s_{apr,lat}$ represents the projection onto the lateral component for the n-th ranging source and $s_{apr,vert}$ the projection of the vertical component and of the along-track component into the vertical for the same n-th ranging source as defined in Equation (17) and σ^2 represents the standard deviation of the uncertainty of the residual differential pseudorange error for the satellite n.

The protection levels in the case of a fault in one of the measurements from the ground receiver are defined for each receiver as

$$VPL_{H_1}[k] = \left|B_{k,apr,vert}\right| + k_{md}\sqrt{\sum_1^N s_{apr,vert,n}^2 \cdot \sigma_{H_1,n}^2} \tag{21}$$

$$HPL_{H_1}[k] = \left|B_{k,apr,lat}\right| + k_{md}\sqrt{\sum_1^N s_{apr,lat,n}^2 \cdot \sigma_{H_1,n}^2} \tag{22}$$

Where k is the index for the ground reference receiver and k_{md} represents the missed detection multiplier, $\left|B_{k,apr,vert}\right|$ and $\left|B_{k,apr,lat}\right|$ are projection of the B-values onto the vertical and lateral component. The B-values are an estimate of the error contribution from each reference receiver to the corrections provided to the aircraft. The other variables are the same as defined in Equation (19) and Equation (20).

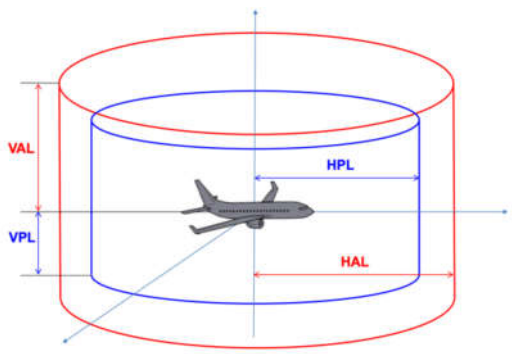

Figure 9, Protection Levels and Alert Limits for the [31]

The maximum of the H_0, H_1 and H_{eph} is then used to compare the PLs with the respective Alert Limit (AL) for a certain position on the approach. The ALs are the maximum allowable NSE for a certain operation and define what an acceptable position error is. Similar to the HPL and VPL, the AL is also expressed in a horizontal and vertical component (HAL and VAL respectively) as seen in Figure 9. As long as the values of the PLs, derived from the augmentation signal and satellite pseudorange

measurements, remain smaller than those of the ALs, integrity is assured, and a safe operation of the aircraft is guaranteed The ALs are shown in Table 4. Additional to the ALs, integrity of an operation is assured through the introduction of the Time to Alert (TTA), which is the maximum allowable time elapsed from the onset of the navigation system being out of tolerance until the equipment enunciates the alert [31]. The TTA for a certain operation is given in Table 2.

Typical operation	**Horizontal Alert Limit (HAL)**	**Vertical Alert Limit (VAL)**
En-route (oceanic / continental low density)	7.5 km	N/A
En-route (continental)	3.7 km	N/A
En-route (terminal)	1.85 km	N/A
Non-Precision Approach	556 m	N/A
Approach operation with vertical guidance (APV-I)	40 m	50 m
Approach operation with vertical guidance (APV-II)	40 m	20 m
Category I Precision Approach (CAT-I)	40 m	35 to 10 m

Table 4, Horizontal and Vertical Alert Limits for GNSS operations.

4.3.3 Continuity

According to the ICAO, continuity is defined as *"the capability of the system to perform its function without unscheduled interruptions during the intended operation." (ICAO Annex 10) [29]*

More specifically, the continuity of a system is the probability that the specified system performance will be maintained for the duration of a phase of operation, presuming that the system was available at the beginning of that phase of operation. This parameter is introduced to ensure a continuous quality of service without unscheduled interruptions.

4.3.4 Availability

ICAO defines the availability of GNSS as *"the portion of time the system is to be used for navigation during which reliable navigation information is presented to the crew, autopilot, or other system managing the flight of the aircraft." (ICAO Annex 10) [29].*

Availability describes the probability that the navigation system will be operational during a certain time. A navigation system is considered available for use in a specific flight operation if the PLs it is providing are inferior to the corresponding specified ALs for that same operation (see Figure 10). The red airplane shape represents the actual aircraft position and the distance from this shape to the centre of the circumferences represents the NSE. The availability is a function of both the physical characteristics of the environment and the technical capabilities of the transmitter facilities [31].

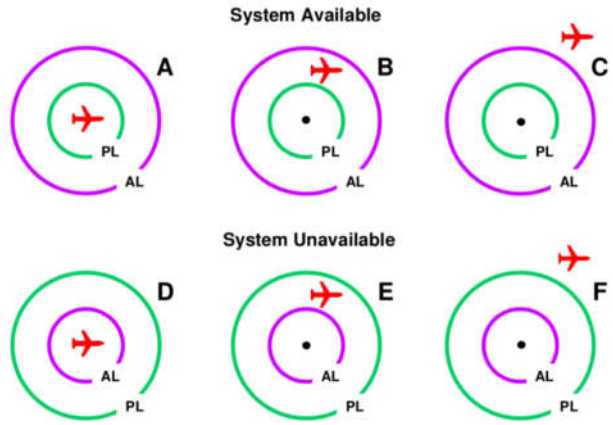

Figure 10, Integrity and Availability Definition [31]

5 Evaluation at Zurich Airport

In September 2019, the DLR conducted experimental flight tests around Zurich Airport with the GBAS-capable Airbus A320 “ATRA” research aircraft (see Figure 11). “ATRA” stands for Advanced Technology Research Aircraft and is the DLR’s largest fleet member. [31] During the five-day flight test period, the aircraft was based in Dübendorf Air Base (LSMD) and conducted around 70 test flights at Zurich Airport. Besides the GBAS tests, other experimental technology was investigated, such as the Low Noise Augmentation System (LNAS), which is mainly focused on noise abatement.

Figure 11, Airbus A320 "ATRA" used for the flight test. [32].

5.1 Test Flight Path

Figure 12 shows the flight path of the test aircraft during around an hour of testing, which is the period that is investigated in this work. It shows multiple approaches into LSZH’s runway 14 conducted from northwest with go arounds performed, followed by left turns back into northern direction in order to repeat the approach procedure. The locations of LSZH and LSMD are marked in red.

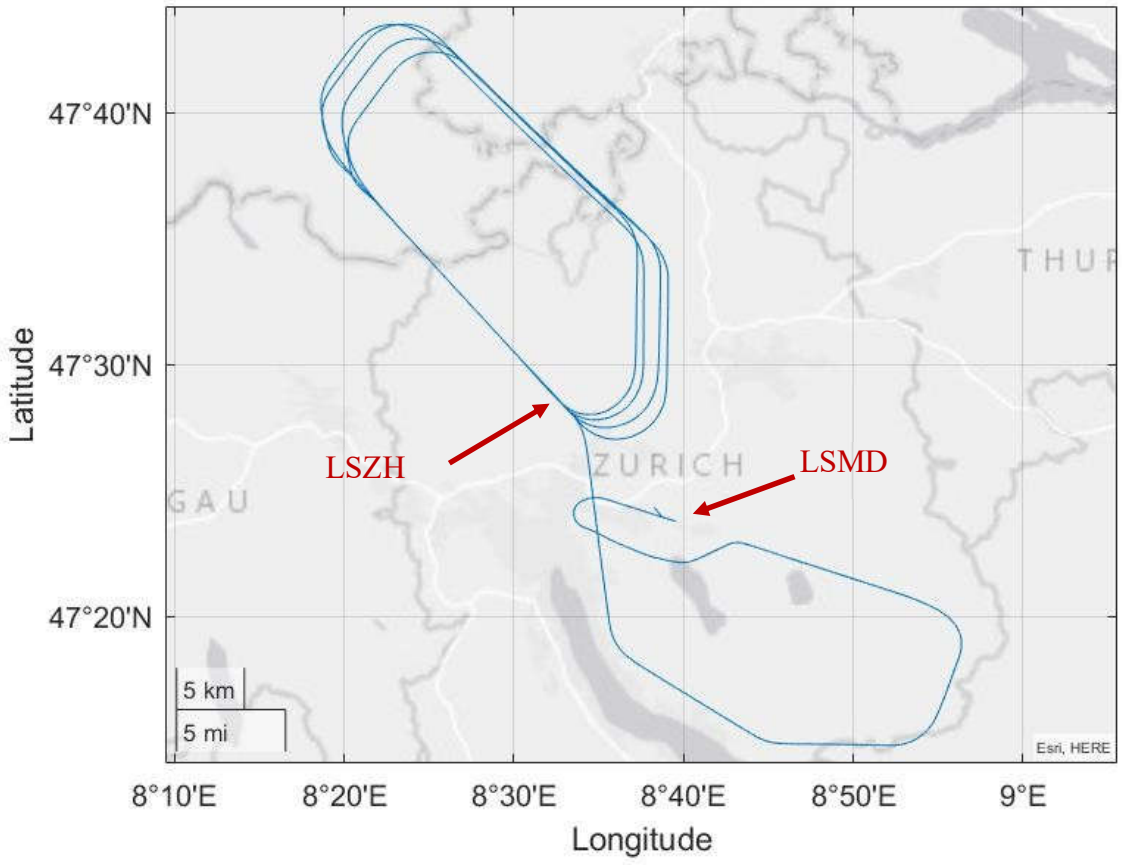

Figure 12, Flight Path of the test flight.

5.2 PEGASUS Program

For the data evaluation in this work, the program PEGASUS (short for Prototype EGNOS and GBAS Analysis System Using SAPPHIRE), developed by EUROCONTROL, was used to decode GNSS data and to perform a GNSS navigation solution. The PEGASUS software user manual describes the program's functionalities and features, which allow the user to evaluate the performance of satellite navigation signals in space as well as their augmentation [33].

The general interface in Figure 13 is divided into three main parts

- Start Scenario
- Graphical Results
- Batch Processor Status

to processes and visualize data. In addition, the status is continuously displayed during processing. This part is the automated way which is intended to simplify data processing. For this work, this was not used, we could directly select the converter in the "Start Standalone Program" area, which will be explained in the next section. The "Start Standalone Program" part is intended for manual processing.

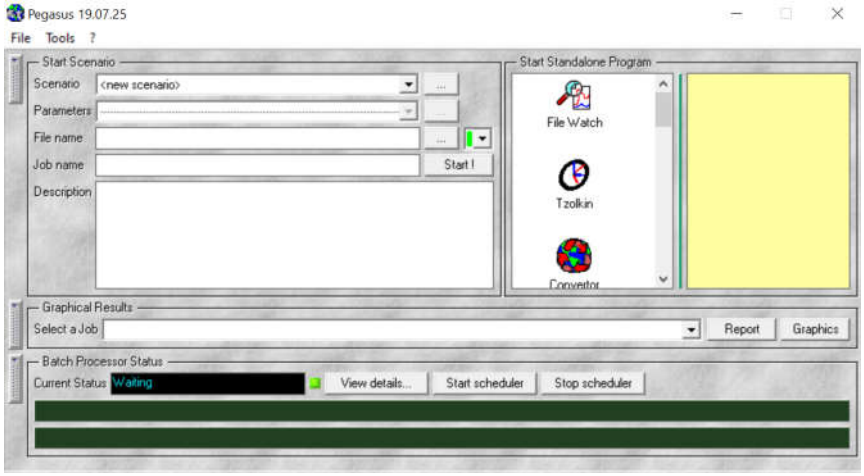

Figure 13 PEGASUS general interface.

5.2.1 Converter

In the first step the converter program as seen in Figure 14 is used to convert the receiver native GNSS data into a standard format. As input for the converter, a RINEX (Receiver Independent Exchange Format) file containing binary data from GNSS receiver is used. The RINEX format is a receiver-independent data storage and exchange format, that contains the pseudorange measurements from the carrier phase observations and the ephemeris data. This data is then converted to a readable ASCII (American Standard Code for Information Interchange) file.

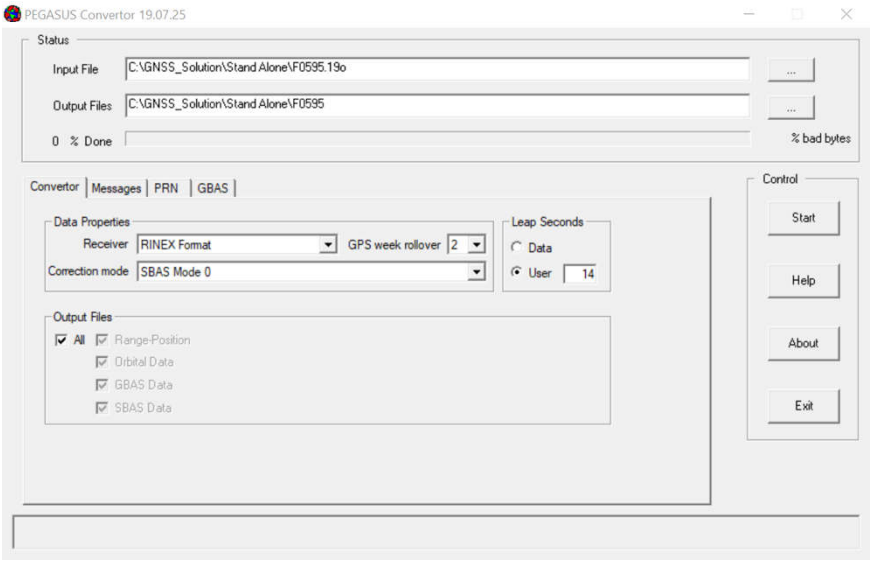

Figure 14, PEGASUS Module Converter.

5.2.2 GNSS Solution

In a next step the GNSS Solution program as seen in Figure 15 is used. The standard format from the converter is used as an input to calculate the GNSS standalone position solution for the user. Furthermore, the program is able to calculate the GBAS corrected solution by adding the corresponding GBAS message as input to "External Messages". The relevant outputs for this evaluation are the GBAS position solution as well as the PLs.

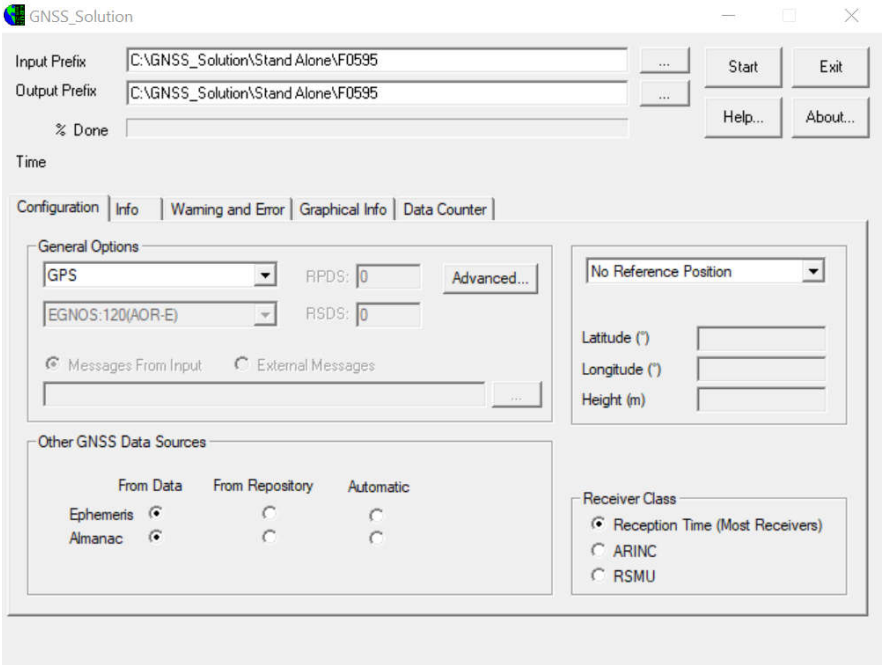

Figure 15, PEGASUS Module GNSS Solution.

5.2.3 File Watch

The FileWatch Module as seen in Figure 16 can be used to visualize results. The module is especially useful to get a quick insight into the data, especially after calculating a position solution. It can be quickly assessed whether the outputs are realistic or not. Additionally, certain values can be extracted from the data in order to further analyse them. In Figure 16, the flight path of the aircraft during the test period is visualized with the position's corresponding elevation shown in colour.

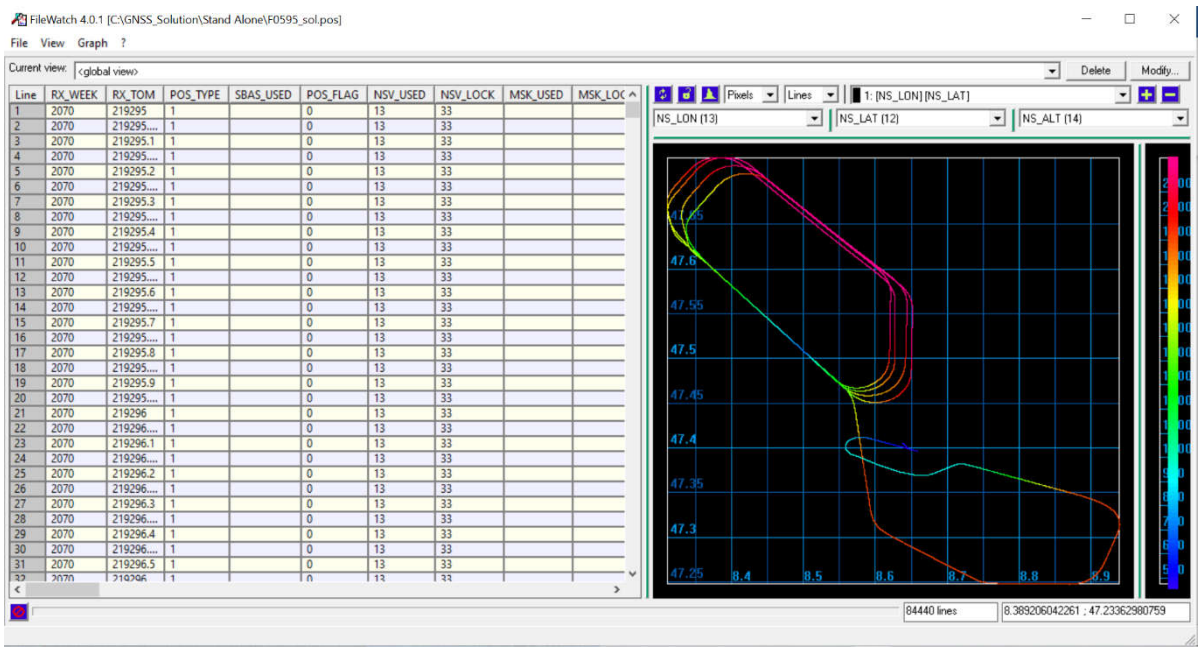

Figure 16, PEGASUS Module FileWatch.

5.3 Accuracy of Standalone GPS

Figure 17 represents the GBAS reference receiver position calculated by standalone GPS (blue) relative to the known GBAS reference receiver position (red) in the horizontal plane. This shows the position solution error that can occur in the standalone GPS position solution as a possible result of atmospheric propagation, multipath effect or adverse satellite geometry as described in Chapter 3, GNSS Error Sources. It is clearly visible that the majority of the data points in the horizontal plane are in the range of 2 m around the actual antenna position, although there are three outliers in the range of 10 to 15 m. The standard deviation in the horizontal plane is 0.3140 m.

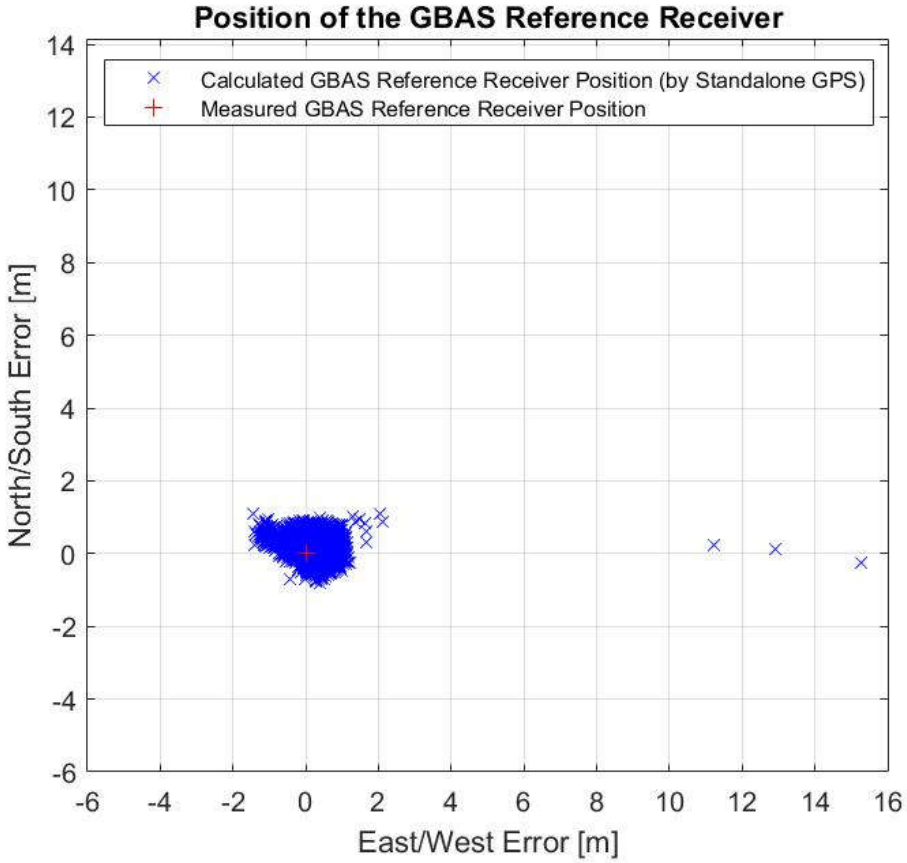

Figure 17, Position of the GBAS Reference Receiver calculated by Standalone GPS, relative to the true location of the GBAS Reference Receiver.

Figure 18 represents the frequency of the vertical error of the GBAS reference receiver position calculated by standalone relative to the known GBAS reference receiver position. It can be derived that the vertical errors range from around minus 4 m to over 35 m, while the majority of the errors are in the minus 2 m to 2 m range. The standard deviation in the vertical is 0.8257 m, therefore representing a larger spread of the position solution error in the vertical axis, compared to the horizontal plane. The standard deviation in the 3-dimensional is 0.6328 m.

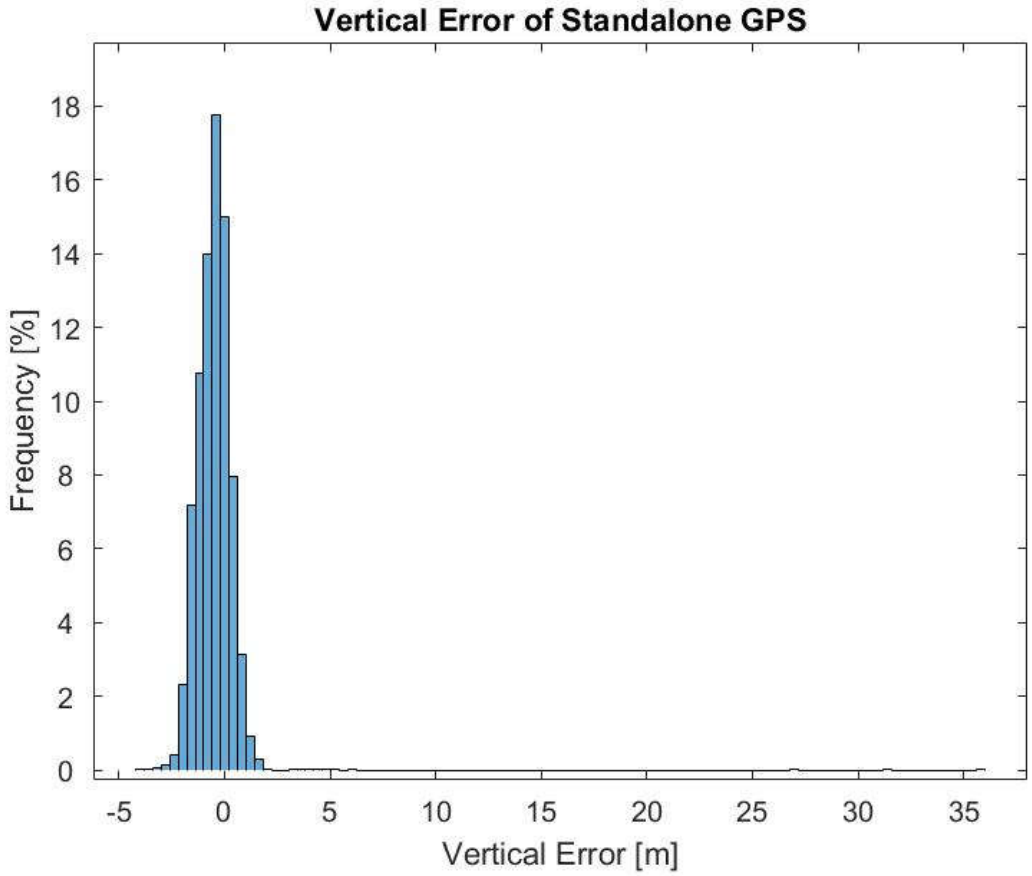

Figure 18, Vertical Error Frequency and Value of Standalone GPS.

Similar to the outliers in the horizontal plane, the data also shows outliers in the vertical. As derived from the data, the reason for these outliers is the initialization process. During this process, the PEGASUS program initializes the processing for the data, therefore leading to incorrect position solutions computed by the program during the first few calculations. The position solutions during this process can be neglected, since it doesn't represent the actual position solution that was determined. Table 5 shows the East/West, North/South and Vertical Errors of the calculated GBAS reference receiver position by standalone GPS and the number of satellites used at the beginning of the initialization process by the program.

East/West Error of calculated GBAS reference receiver position	North/South Error of calculated GBAS reference receiver position	Vertical Error of calculated GBAS reference receiver position	Number of satellites used
NaN	NaN	NaN	0
NaN	NaN	NaN	0
NaN	NaN	NaN	1
NaN	NaN	NaN	1
NaN	NaN	NaN	1
NaN	NaN	NaN	1
NaN	NaN	NaN	1
NaN	NaN	NaN	2
NaN	NaN	NaN	2
NaN	NaN	NaN	2
NaN	NaN	NaN	2
NaN	NaN	NaN	2
NaN	NaN	NaN	3
12.9023509762192	0.131051791186110	31.5088544798000	4
11.2051472278836	0.252711536859351	27.0509893301000	4
15.2698633164619	-0.241117027940163	35.9769688521000	4
2.03935943227407	1.10498581170759	5.92220452729998	5
2.13188250745588	0.867396670855669	5.40129218089999	5
1.66598465966672	0.308632756514271	3.64246289360000	5
1.65028393621469	0.609236175705519	4.02729856249999	5

Table 5, East/West, North/South and Vertical Error of calculated GBAS reference receiver position and number of satellites used.

In general, it can be said that in terms of the static GBAS reference receiver position calculation, standalone already shows an accuracy mostly in the range of around 2 m. The problem with standalone is that the integrity, continuity and availability is not assured, therefore the performance is insufficient for critical operations such as CAT-I precision approaches.

5.4 Comparison of standalone and GBAS-corrected flight path

Figure 19 shows the flight path of a smoothed standalone position solution (blue line), and the GBAS-corrected flight path (red line). The behaviour of the standalone flight path shows an unsteady movement around the GBAS-corrected flight path. The deviation in this case is mostly in the decimetre range, but it is still visible that the GBAS system has a higher stability by showing a straighter line. This behaviour is shown over the whole flight path with some exceptions, which will be discussed in the next chapter.

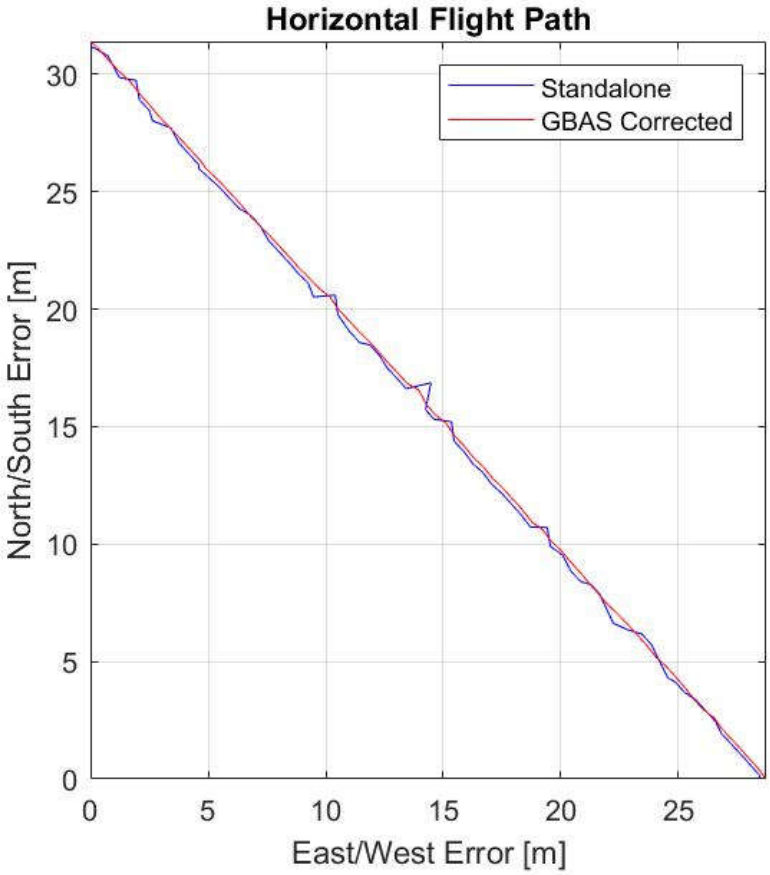

Figure 19, Example of a GBAS Position Solution and a Standalone Position Solution for the same Flight Path.

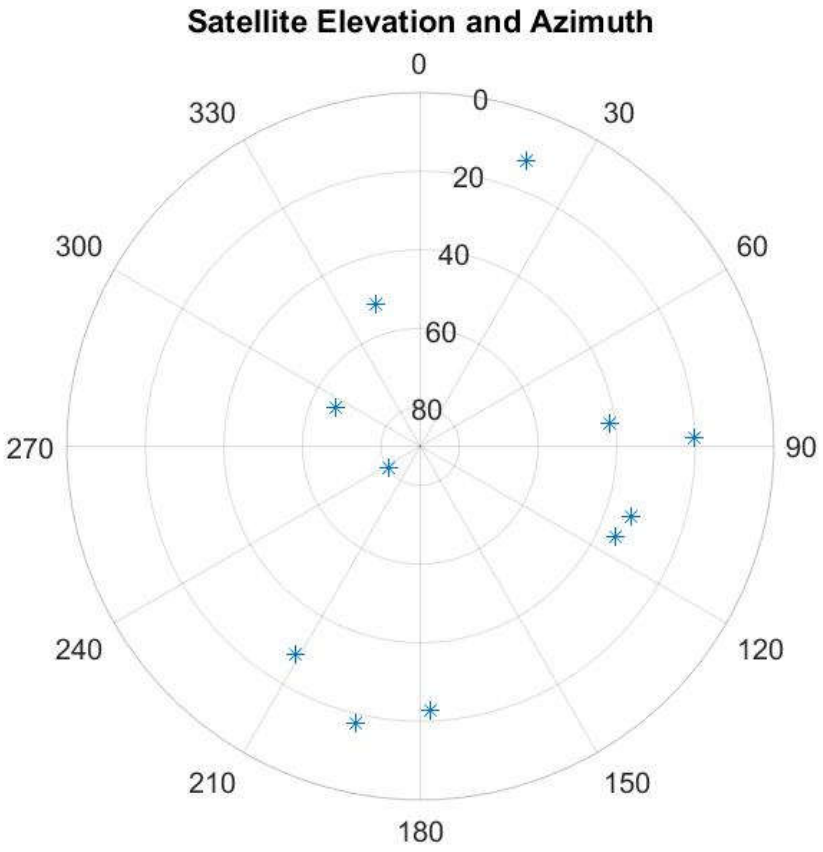

Figure 20, Skyplot of the used Satellite Geometry during the flight path seen in Figure 19.

The skyplot as seen in Figure 20 is the satellite geometry used for the flight path computation from Figure 19. Concentric circles represent satellite elevation angles (the vertical angle with respect to the horizon) and the outer angular axis represent the satellite azimuth angles (the horizontal angle in respect to the cardinal direction north). It shows a strong geometry with 11 satellites used, with satellites distributed in different elevation angles and different azimuth angles. It is important to note that the skyplot only provides a great first impression for the satellite geometry, although it is not fully representative for the quality of the position solution computation. The S-Matrix, as described in Equation (16) remains the important representation of the quality of the position solution computation.

5.5 Protection Levels

As described in Chapter 4.3, GBAS Performance Characteristics, the PLs are an indicator for the performance, precisely the integrity, of a GBAS-corrected position solution. Basically, it can be said that the higher the PLs, the lower the integrity of the calculated position solution. Figure 21 and 22, respectively, show the VPLs and HPLs during the test period, with PL peaks marked with numbers. Table 6 lists the peak values with its corresponding time stamps, HPL and VPL values and number of satellites used, as well as their previous and subsequent two data points as reference. Taking a look at the number of satellites that are used for the GBAS-corrected position solution during the peaks in the PLs, it can be concluded that a sudden drop in the number of satellites used leads to an increase in the PLs. Therefore, a correlation of the number of satellites used and the performance of GBAS can be assumed, confirming the fact that the number of satellites available has a direct impact on the performance of GBAS, as described in Chapter 3.5, Satellite Geometry. Additionally, the s_{vert} and s_{lat} values increase, leading to a higher impact of a pseudorange measurement error by a single satellite on the position solution.

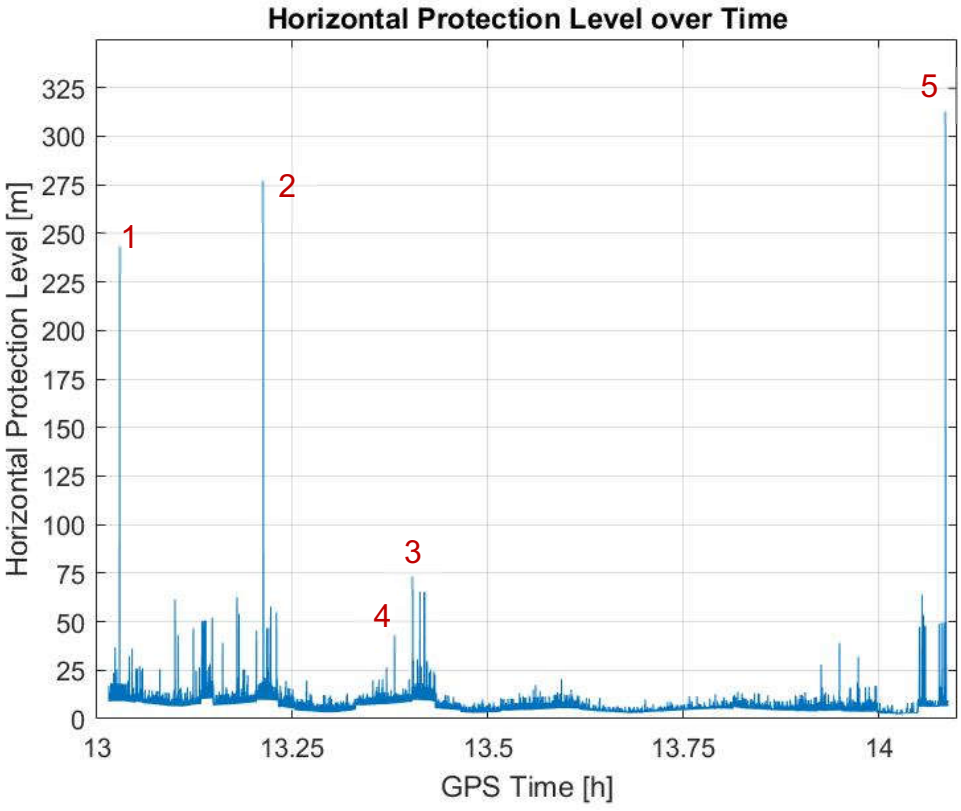

Figure 21, Horizontal Protection Level for the test period.

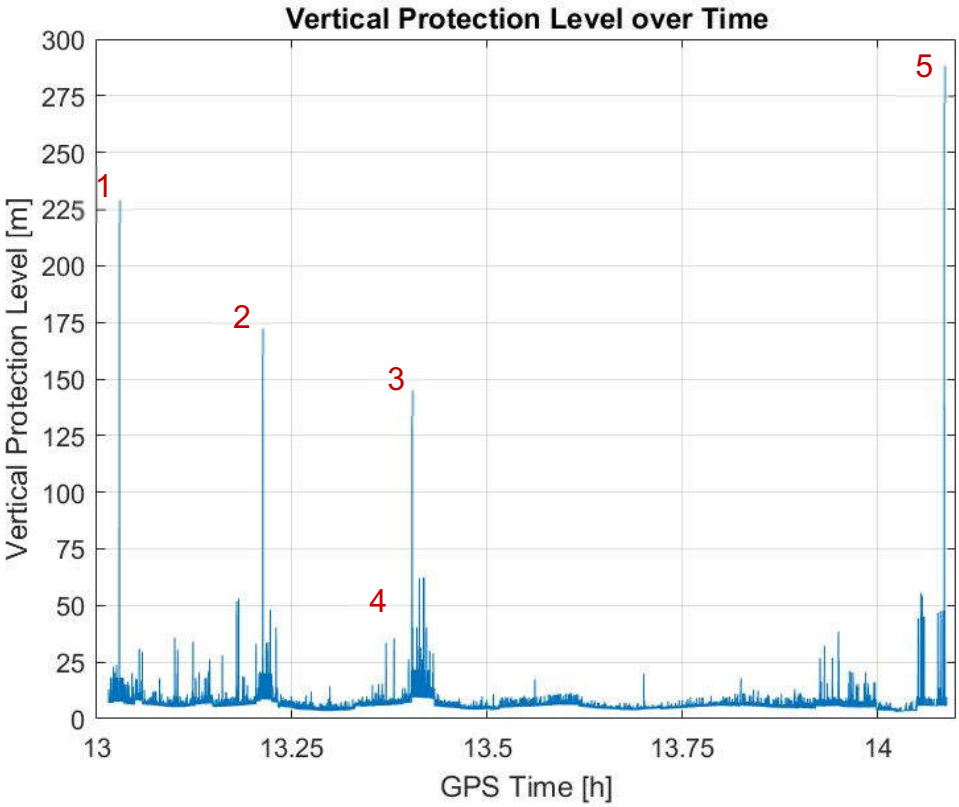

Figure 22, Vertical Protection Level for the test period.

Peak number	GPS seconds of week [s]	HPL [m]	VPL [m]	Satellites used
	219704.3	13.8302	12.8566	5
	219704.3.5	12.4348	10.2463	6
1	219704.4	**243.437**	**229.207**	**4**
	219704.45	127.31	118.466	5
	219704.5	9.15085	7.56626	7
	220356	10.0593	8.7794	6
	220356.05	10.0606	8.78058	6
2	220365.1	**277.286**	**172.599**	**4**
	220356.15	12.1145	10.2893	6
	220356.2	9.76966	8.57511	7
	221053.3	9.70439	9.33332	7
	221053.35	16.6868	21.5359	6
3	221053.4	**73.4842**	**145.14**	**4**
	221053.45	9.70872	9.33762	7
	221053.5	9.70597	9.33512	7
	220253.65	7.75818	5.76057	9
	220253.7	8.80165	6.91081	8
4	220253.75	**54.0042**	**53.0304**	**4**
	220253.8	7.74567	5.7514	9
	220253.85	7.76112	5.76277	9
	223505.9	7.75818	5.76057	6
	223505.95	-	-	12
5	223506	**313.419**	**288.304**	**4**
	223506.05	6.45491	5.77242	6
	223506.1	6.45176	5.76953	6

Table 6, Timestamp, HPL, VPL and number of satellites used during peaks in the Protection Levels.

It is evident that during the peaks 1 to 5 from Table 6, the number of satellites used intermediately drops to four, before increasing again. Nevertheless, the values of the PLs during those four peaks strongly differ from each other, with peak 4 being the lowest, and peak 5 being the highest value for the VPL and the HPL. The reason for the difference in peak values can be explained through the different satellite geometries during the point of observation as seen from the receiver. The gathered data shows a gap in the HPL and VPL values in the timestamp before peak 5. The reason for this gap in the data set is unknown and will be further investigated by the PEGASUS team.

Figure 23 shows the four occuring satellite geometries as seen from the receiver for PL peaks 1 to 4 in a skyplot.

- The skyplot for peak 1 shows that the four satellites are in a straight line, therefore generating high s_{vert} and s_{lat} values due to the weak satellite geometry.
- The skyplot for peak 2 shows that three out of four satellites used are in an azimuth area of 210 to 240 degrees, therefore also generating a weak geometry and high s_{vert} and s_{lat} values.

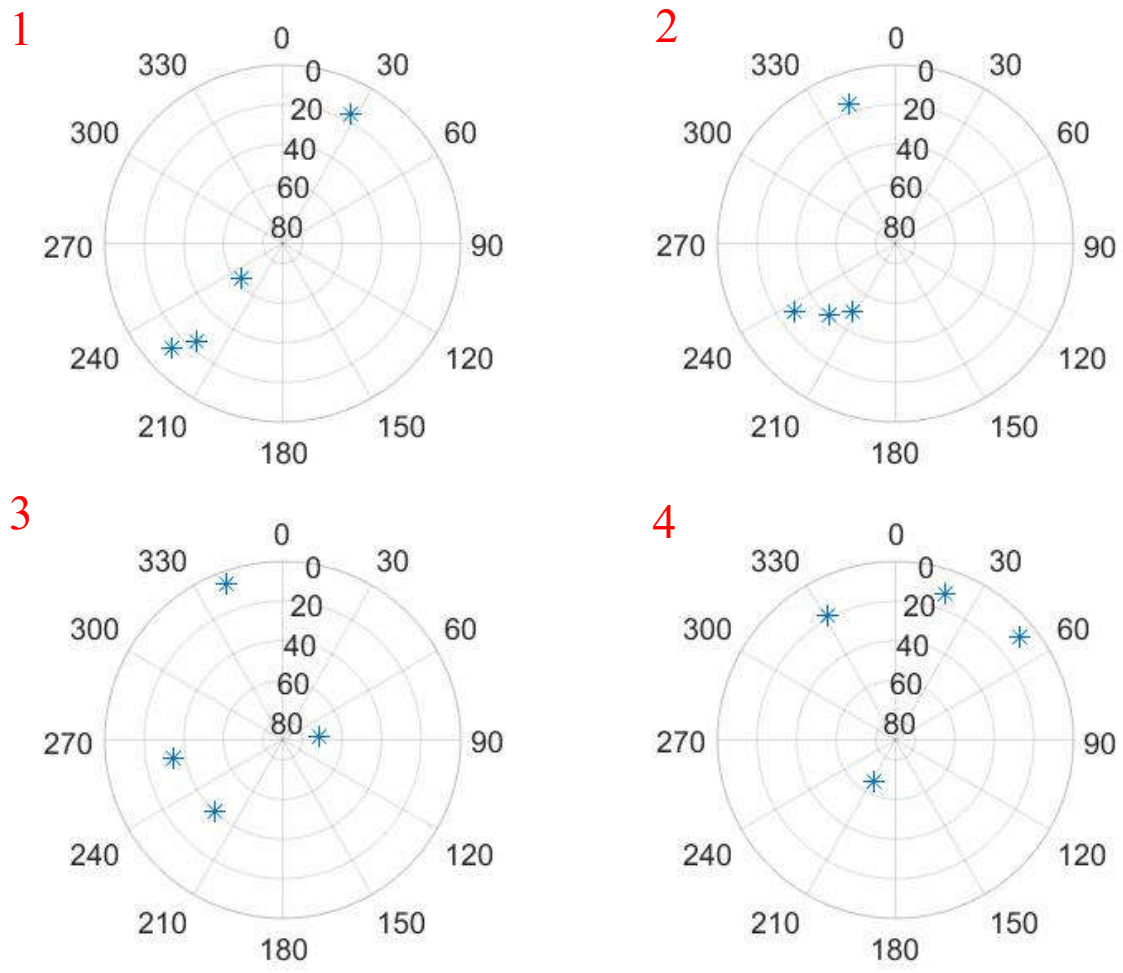

Figure 23, Skyplots with the used satellite geometry during Protection Level peaks 1 to 4.

- The skyplot for peaks 3 and 4 show similar geometries, which are stronger than the ones seen in the skyplots for peak 1 and 2. Compared to peak 4, the elevation angle of most of the satellites seen in peak 3 are higher, leading to an assumed less ideal geometry in the vertical, and therefore to a higher VPL than at peak 4. The reason for the PL peaks 3 and 4 being lower than the PLs at peaks 1 and 2 might be due to a more distributed set of satellites as seen from the receiver, therefore generating lower s_{vert} and s_{lat} values than the ones derived from peaks 1 and 2.

Figure 24 represents the PLs with the corresponding number of satellites used. As described previously, the number, as well as the geometry of the satellites used have a direct impact on the PLs. This relation is visible, where in general, the more satellites are used for the position solution, the smaller both the VPL and HPL become. Additionally, as also seen in Figure 24, it is also evident that the peak values vary depending on the strength of the satellite geometry.

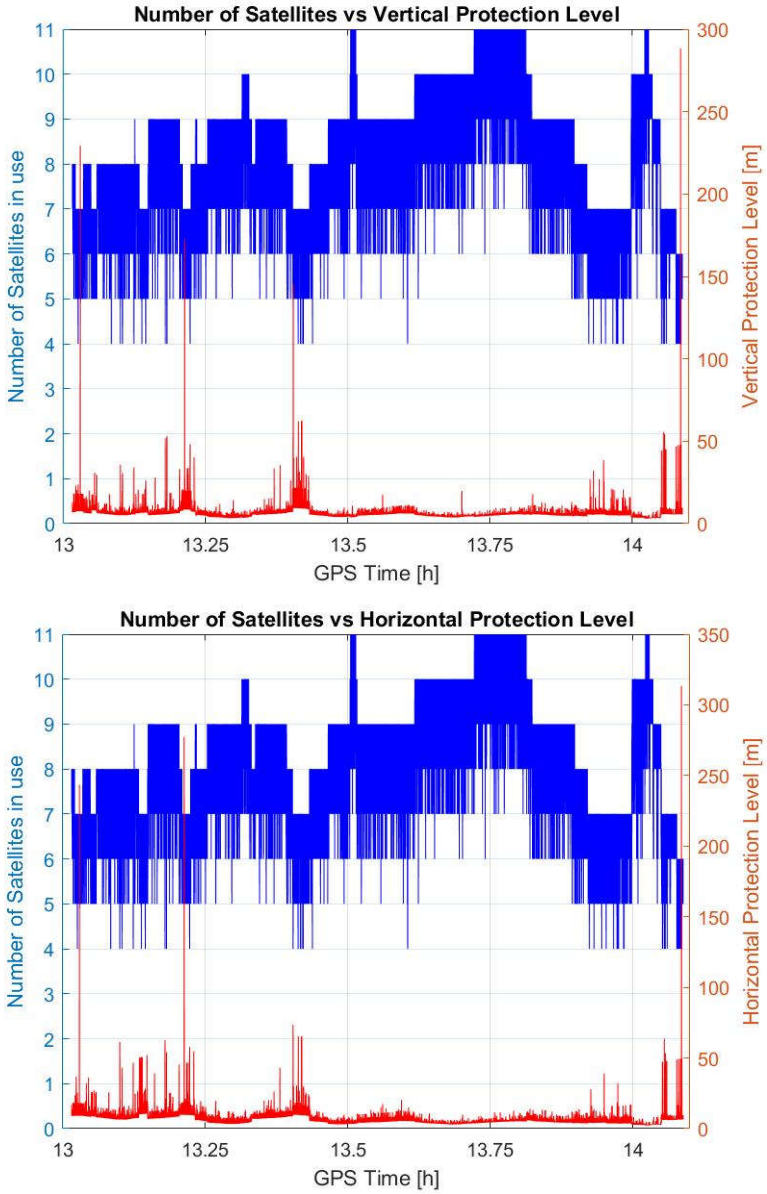

Figure 24, Number of satellites vs. Vertical and Horizontal Protection Level during the test period.

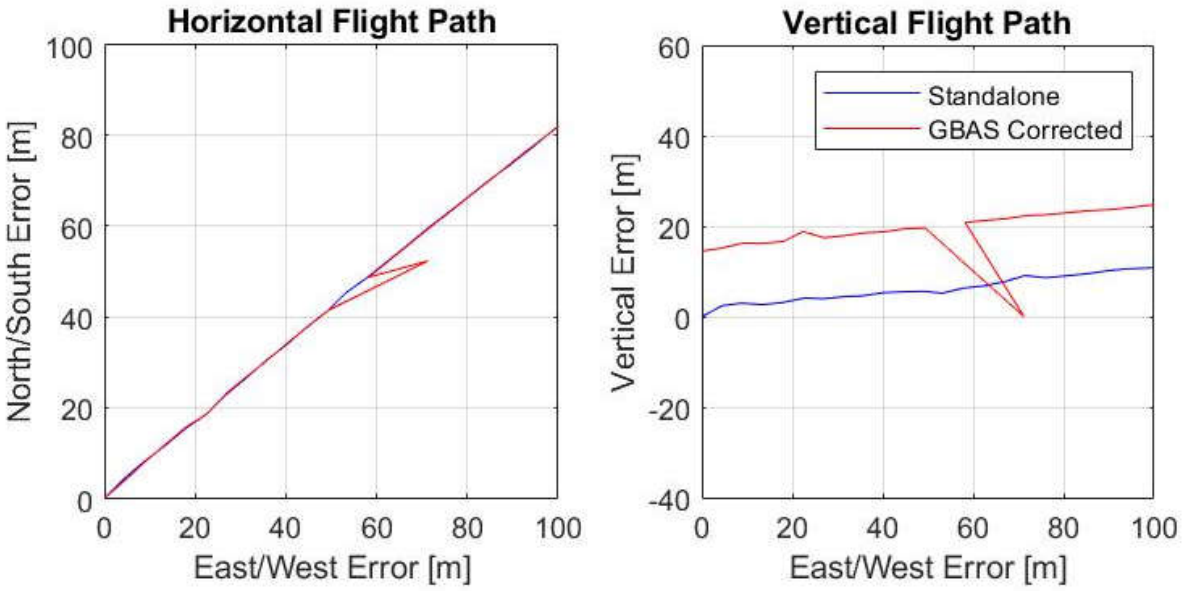

Figure 25, Vertical and Horizontal Flight Path which corresponds to the second peak in the Protection Level.

In this section, the effects of the peaks in the PLs on the flight path is analysed. The horizontal and the vertical flight path corresponding to the time stamps of peak 2 is seen in Figure 25, where the zero positions of the axes represent the start of the GBAS-corrected flight path in this extract. There is a clear outlier in the GBAS-corrected flight path (red line), which represents the position solution for the aircraft during the peak 2 of the PLs (see Table 6 for the corresponding PL values). It is important to note that the standalone and GBAS-corrected vertical flight paths differ strongly from each other. While the horizontal flight paths are more of less identical (except the outlier of the GBAS-corrected flightpath), the vertical flight paths constantly differ in the magnitude of about 15 m. A reason for this might be that there are no satellites available below the user for the position solution. Satellites would have to have an elevation angle between 0 and 90 degrees measured from the horizon upwards, as well as an elevation angle between 0 and 90 degrees measured from the horizon downwards as seen from the user location. The latter is not possible due to the earth's geometry. This means that there is a significantly lower depth for the vertical position solution compared to the horizontal position solution, leading to a less accurate flight path representation.

The outlier in the GBAS-corrected flight path raises the question why the standalone position solution is assumed to be more accurate than the GBAS-corrected position solution in this case. The data shows that more satellites were available for the standalone-calculated flight path than for the GBAS-corrected flight path calculation. Specifically there are 5 satellites used for the standalone position solution and 4 satellites used for the GBAS position solution. This behavior can also be observed for the other peaks 1,3 and 4. A reason for this might be the integrity monitoring of GBAS, where satellites can be excluded from the computation of the position solution, if they broadcast faulty data. Nevertheless, by excluding one satellite from the position solution (4 satellites instead of 5), it should not lead to such an outlier in the position solution. Therefore, this case will be further investigated by the PEGASUS team.

5.5.1 Protection Levels vs. Alert Limits

The availability, as seen in Chapter 4.3.4, Availability, is given, when the PL values remain smaller than the AL values during 99% to 99.999% of the time. The percentage is dependent upon several factors including the intended operation, traffic density, and complexity of airspace and availability of alternative navigation aids.

As seen in Figure 26, the HPL exceeded the HAL five times during the test period. The reason for the ALs not remaining constant is the different requirement for ALs for different operations, as seen in Table 4. The four incisions represent the aircraft's final approach phase. For the HPL, 5 out of 77233 HPL computations for this certain test-period are above the HAL, therefore inidcating an availability of 99.99 %. For the VPL as seen in Figure 27, 23 out of 77233 VPL computations for this certain test period are above the VAL, therefore indicating an availability of 99.7 %.

If the HPL or VPL exceed the HAL or VAL, respectively, no actions in terms of warnings sent to the primary flight display or flight computer are taken, as long as the excess is not longer than the Time to Alert at this current type of operation, as described in Table 4. Since, during this test period, no exceedings last longer than the Time to Alert during the type of operation at this moment, the pilot does not receive any warnings, but rather notices a gap in the guidance providance during the exceeding.

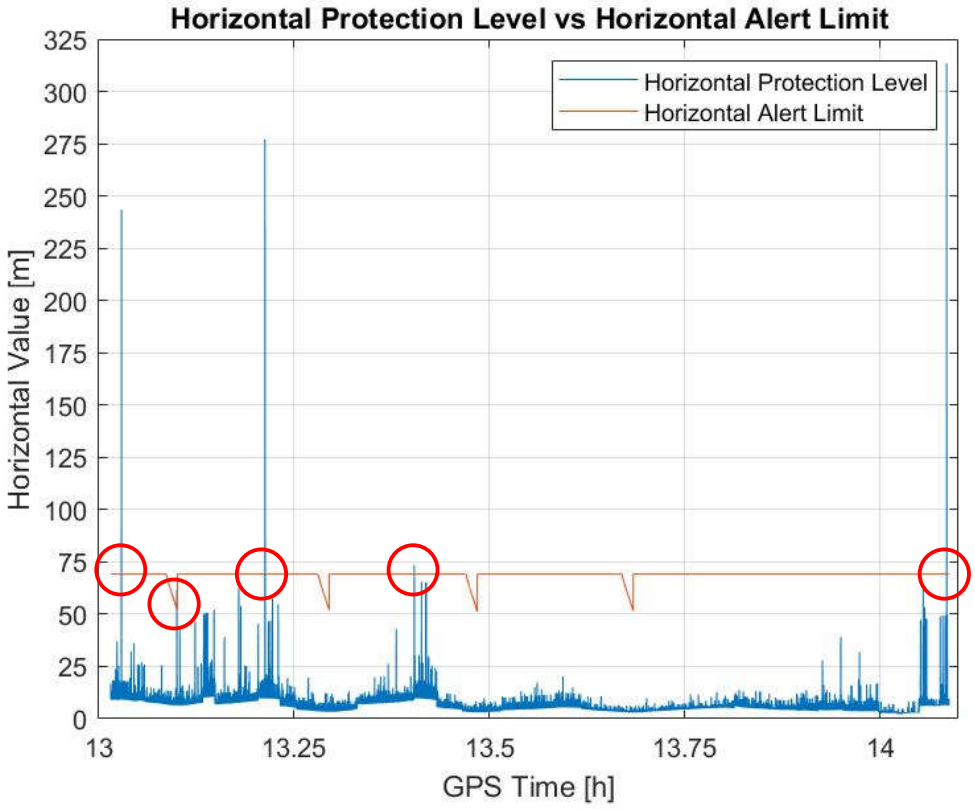

Figure 26, Horizontal Protection Levels and Horizontal Alert Limits during the test period.

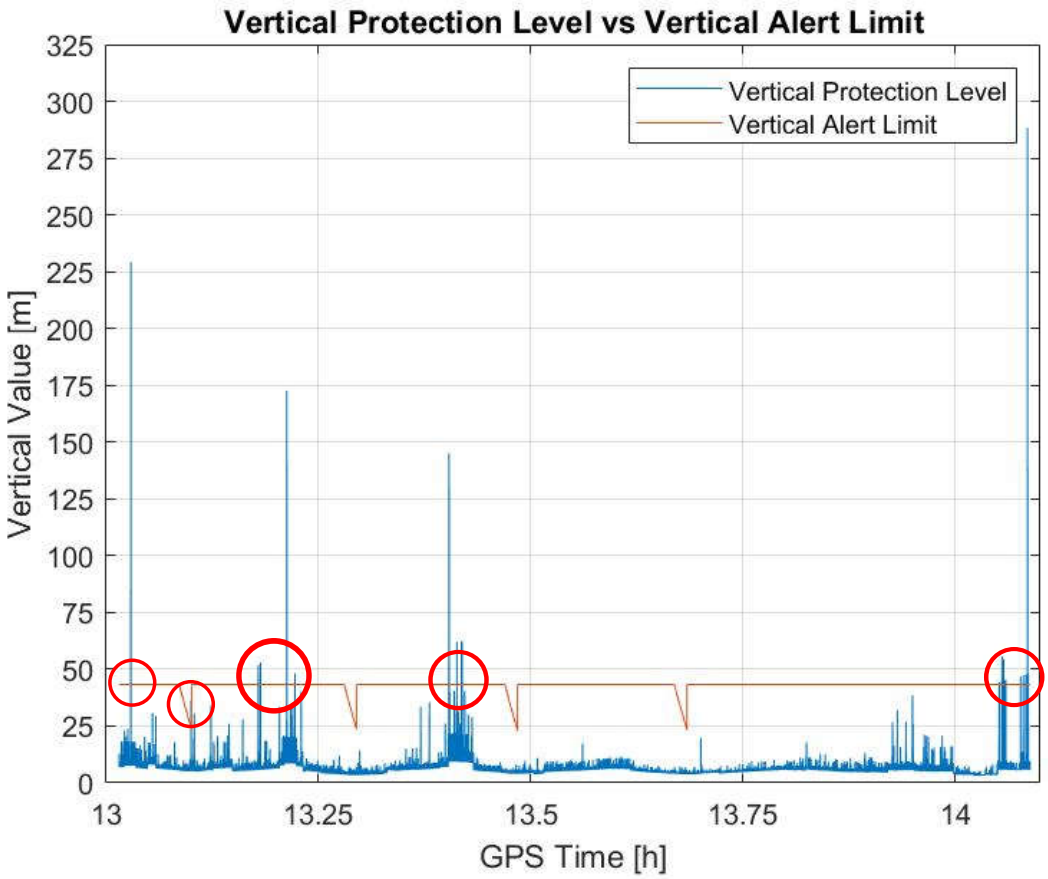

Figure 27, Vertical Protection Levels and Vertical Alert Limits during the test period.

It is important to note that for the actual performance evaluation of an operational GBAS, the investigated test period of around an hour is insufficient to formulate accurate conclusions. Therefore, the availability assessment is not representative for the true performance of the GBAS at LSZH, but rather shows the performance of this roughly hour-long test period.

5.6 Difference of standalone relative to GBAS

Figure 28 shows the difference of the standalone position solution (blue "x") relative the GBAS corrected position solution (red "+" at (0,0)). It is important to note that although GBAS is presented as the true and exact position solution, in reality it also shows some deviation from the true position of the user. Overall, the standard deviation is 0.4001 m in the horizontal plane. This value is rather small and implies that standalone has good accuracy most of the time compared to GBAS. But still many larger deviations are visible, which are assumed to be originated by error sources that are explained in Chapter 3, GNSS Error Sources. Compared to the standalone case, most of these errors are corrected in the case of GBAS.

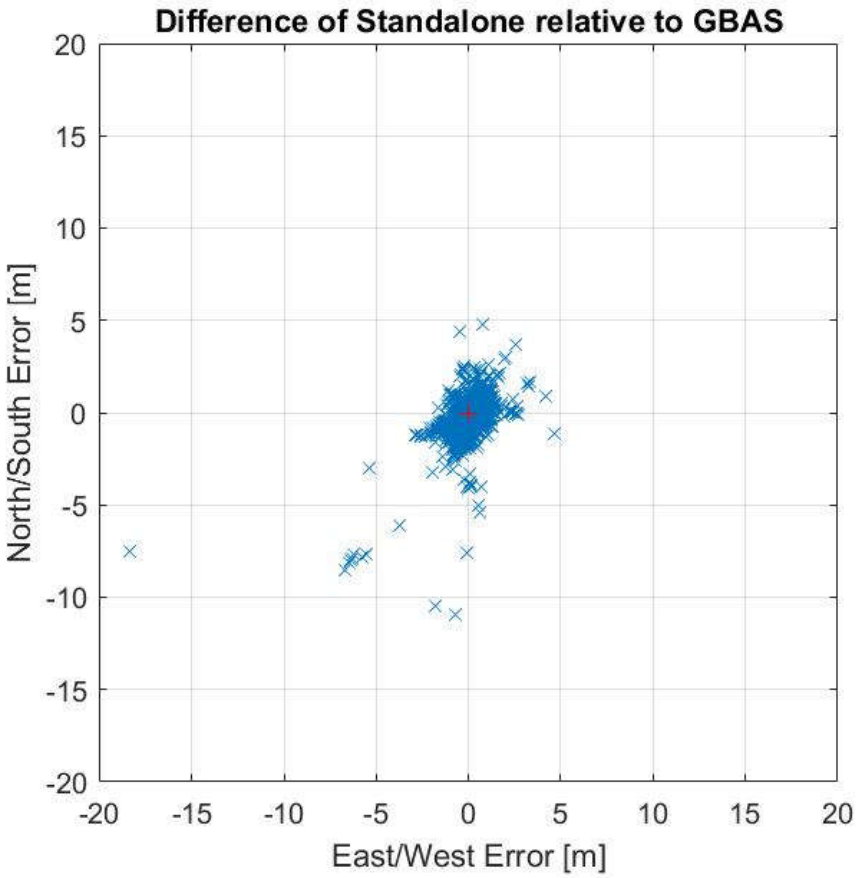

Figure 28, Difference of Standalone position solution compared to GBAS corrected position solution in the horizontal plane.

Figure 29 shows the vertical difference of the standalone position solution relative to GBAS, which is in the coordinate zero point as reference. It is visible that there is a wider spread in the direction of the vertical axis compared to the spread in the horizontal plane. The standard deviation for the vertical axis is 0.9963 m. In addition, it is noticeable that the histogram is right-skewed and therefore the majority of the position solution is below the reference position of the GBAS-corrected position solution. A reason for this is assumed to be that there are no satellites available below the user for the position solution, as already discussed in the evaluation of Figure 25.

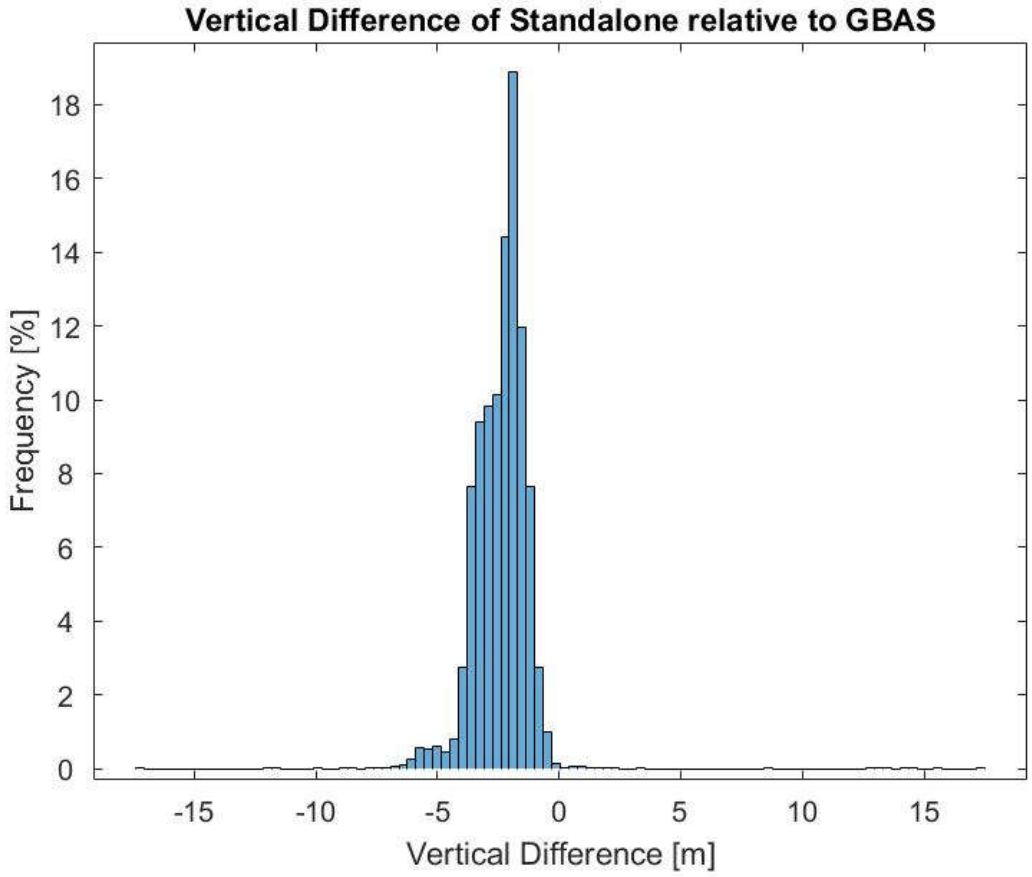

Figure 29, Histogram of the vertical difference of Standalone position solution compared to GBAS corrected position solution.

The total standard deviation in the 3-dimensional is 1.3309 m, which is larger than the standard deviation of 0.6328 m for the standalone relative to the measured location of the GBAS reference receiver as seen in Chapter 5.3, Accuracy of Standalone GPS. A few assumptions for this difference are given below:

- The reference receiver is at a known location, whereas the GBAS-corrected flight path does not represent the true location of the aircraft, since the errors are not completely eliminated by GBAS.
- The aircraft is in a dynamic state, whereas the GBAS reference receiver is in a static state. Therefore, there might be more errors introduced through the movement of the aircraft.
- The sophisticated receiver in the GBAS reference antenna differ from the receiver used on the aircraft.

6 Conclusions and Final Remarks

In this chapter, the summary and conclusions for this work are discussed, and further proceedings are proposed.

6.1 Summary

This work focused on the use of satellite navigation technology in civil aviation, particularly on the GBAS for CAT-I precision approaches.

It starts by giving an overview of the background of GBAS, with a discussion of the current standard precision approach guidance ILS. A review of the operating principle and different approach categories gives an idea on the general functionality of approach guidance. The vulnerability to signal reflections or distortions by preceding aircraft or obstacles in the vicinity reveals the downsides of an ILS. Its limitation of only providing uniform, straight-in approach guidance is discussed, promoting the implementation of a GBAS Landing System.

Subsequently, a brief discussion of GNSS is given, supplemented with a review of the GNSS core constellations, namely the GPS, GLONASS, BeiDou-2 and GALILEO. Then, the derivation of the navigation equations used for the position solution is given, explaining the pseudorange measurement equations, the carrier phase equation of the signals, the functionality of carrier-smoothing and the final smoothed pseudorange equation and ultimately the fact that satellite navigation is a 4-dimensional system with time as the fourth dimension. This chapter is concluded with a discussion of the GNSS signals in the L-Band, elucidating the carrier, the ranging code and the navigation data, which characterize the signal components.

The next chapter includes the GNSS error sources, which constitute an important aspect for the satellite navigation and indicate the reason for the necessity of augmentation systems. The largest error source being the ionosphere, which introduces a range error in the pseudorange measurement through the signal propagation by atmospheric refraction. Another similar, but less severe, error source is the signal delay introduced by the troposphere, which depends on the humidity, pressure and temperature of the lowest atmospheric layer. Multipath is an error source that leads to the user's antenna receiving a signal via a mixture of refracted and direct paths, resulting in a distortion of the correlation peak in the receiver when determining the pseudorange. Orbital errors regarding the satellite orbit determination and clock accuracy can lead to errors in the ephemerides, therefore broadcasting incorrect information about the location of a satellite, resulting in a position solution inaccuracy for the user. The chapter is concluded with a discussion of the importance of a strong satellite geometry, which becomes an important aspect in the evaluation of the flight test data at LSZH.

Chapter 4 discusses the GBAS and starts by explaining the purpose of a GLS, being an approach guidance system with greater flexibility compared to ILS and having an economical benefit due to a reduced cost of maintenance by only requiring one ground station per airport. Its infrastructure subsystems, consisting of the satellite subsystem, ground subsystem and aircraft subsystem are discussed. The ground subsystem

receives the standalone GNSS signals, processes and integrity monitors them in the ground facility and transmits the final GBAS data through the VDB transmitter to the aircraft. In the aircraft subsystem, the Multi-Mode Receiver applies the corrections to the pseudorange measurements taken by the GNSS receiver on board the aircraft, in order to gain more accurate GPS position, velocity and time to guide the aircraft safely to the runway. Additionally, the math behind correction generation by the ground and aircraft subsystem is elucidated. This chapter is concluded with the elaboration on the GBAS performance characteristics, containing the four parameters Accuracy, Integrity, Continuity and Availability, which combined, define the main difference in the data output of the GBAS compared to the standalone GPS.

Chapter 5 discussed the flight test data, by first visualising the flight path of the conducted test flight. Then, the program used for the computation of the position solution, PEGASUS, is discussed, followed by an analysis of the accuracy of standalone signals on the position solution of a GBAS reference receiver antenna. The flight paths based on standalone and GBAS-corrected position solutions are compared and the Protection Levels, which define the integrity of GBAS, are discussed. Furthermore, the reason for peaks in the Protection Levels are explained by taking a look at the used satellite geometry during those peaks. Finally, the Protection Levels are compared with the Alert Limits and the difference of standalone relative to GBAS-corrected position solution is analysed.

6.2 Conclusion

The evaluation concludes that the smoothed standalone position solution does indeed already provide accuracy in the magnitude of mostly less than two meters horizontally as well as vertically for the position solution of the GBAS reference receiver as seen in Figure 27 and 28. This is certainly a good performance, regarding the number of error sources that affect the signal, although the receiver antennas' open location, clear of reflective surfaces mitigate the effect of multipath. The standalone GPS' accuracy would not be as decent if the receiver antennas would be located in an urban area, surrounded with reflective surface.

Furthermore, it turns out that the GBAS primarily applies corrections to the vertical plane of the standalone position solution and that the horizontal position solutions are roughly identical in the GBAS-corrected and the standalone case. Additionally, the impact of the satellite geometry on the accuracy of position solutions is confirmed by the comparison of the PLs during different satellite geometry occasions.

It is also evident that the use of the minimum of four satellites required for a position solution can lead to large errors in the accuracy. This confirms the fact that in order to generate an accurate position solution (regardless of using GBAS-corrected or standalone position solutions), the use of more satellites is ideal.

Additionally, it can be seen that GBAS mostly shows a more straight and stable flight path compared to standalone, although there are some outliers in the GBAS position solution. Satellites that lead to inaccuracies in the standalone position solution are excluded from the GBAS position solution by the integrity monitoring of the GBAS ground facility. This might also be a reason for larger peak values of the PLs and

outliers in the GBAS-corrected flight path, since less satellites are used for the GBAS than for the standalone position solution.

Due to unsolved reasons, the test flight data often shows sudden changes in the used satellite geometry and that in general, this data set with a test period of roughly an hour is insufficient for the performance evaluation of GBAS-corrections generated by an operational GBAS. The data set shows a weak performance of the certified and operational GBAS at LSZH, which is why it is not representative for the actual performance of this certain GBAS. There are systematic differences in terms of the receivers and antenna location on the aircraft used for this test period, compared to the aircraft operating commercially. The receiver is experimental and the antenna is located at a position that is more prone to multipath, therefore it can be assumed that those factors might lead to a weaker GBAS performance than expected. Furthermore, the performance in terms of PLs fluctuate strongly, which might be due to the use of less satellites than actually available, which is not expected for an operational GBAS. Therefore, the final conclusion suggests that the data set used for this work shows the worst-case scenario at the most and does not represent the reality.

6.3 Future Proceedings

In order to perform an extensive and accurate evaluation of the performance of a GBAS and comparison of GBAS-corrected and standalone position solutions, it is suggested to use a data set with a longer test period. The period of roughly an hour is simply not enough to assess the performance in all cases. Additionally, the use of an aircraft with a commercial GBAS subsystem rather than aircraft with an experimental GBAS subsystem would evaluate the real performance of daily operations of the GBAS at LSZH. Furthermore, an evaluation under different and dynamic atmospheric conditions such as different states of the ionosphere and troposphere would be feasible to evaluate the performance of the GBAS under different conditions. This is not achieved by using a test period of roughly one hour, where atmospheric influences are more or less constant. This work could be extended by the investigation of anomalies which are assumed to be introduced by the PEGASUS program. This investigation is further conducted by the PEGASUS team and will not be included in this work. Another further proceeding is a comparison of the ILS performance to the GBAS performance. In summary, this work is very specific and many more aspects in the performance evaluation of GBAS and standalone GPS can be considered that would result in a more extensive and realistic performance evaluation.

7 Bibliography

[1] ICAO, “Future of Aviation,” [Online]. Available: https://www.icao.int/Meetings/FutureOfAviation/Pages/default.aspx. [Accessed 8 December 2020].

[2] ETHW, “First-Hand: Development of the Instrument Landing System Glide Path,” 12 Janury 2015. [Online]. Available: https://ethw.org/First-Hand:Development_of_the_Instrument_Landing_System_Glide_Path. [Accessed 8 December 2020].

[3] L. S. a. V. Fritch, “Instrument Landing Systems,” 1973.

[4] Flughafen Zürich, “Neue Flugverfahren,” [Online]. Available: https://www.flughafen-zuerich.ch/unternehmen/medien/aktuelle-themen/neue-flugverfahren. [Accessed 8 December 2020].

[5] M. Felux, “Gastvortrag GNSS,” 2019.

[6] “Wie funktioniert ILS (Instrument Landing System)?,” [Online]. Available: https://antwortenhier.me/q/wie-funktioniert-ils-instrument-landing-system-59898928358. [Accessed 11 September 2020].

[7] ICAO, Standards and Recommended Practices (SARPs) Annex 6, Quebec, 2018, p. 3.

[8] Skybrary, “Instrument Landing System (ILS),” 19 October 2014. [Online]. Available: https://www.skybrary.aero/index.php/Instrument_Landing_System_(ILS). [Accessed 22 September 2020].

[9] M. Felux and H. Becker, “GBAS landing system - Precision approach guidance after ILS,” 2012.

[10] A. Dasgupta, “Evolution of the Global Navigation Satellite Sysytem (GNSS),” *Geospatial World,* 20 September 2016.

[11] C. F. Leroy, “Second International Geodetic Symposium on Satellite Doppler Positioning,” pp. 185-190, June 1979.

[12] T. J. FORD and J. Hamilton, "A New Positioning Filter: Phase Smoothing," 2003.

[13] ESA, “Satellite frequency bands,” [Online]. Available: https://www.esa.int/Applications/Telecommunications_Integrated_Applications/Satellite_frequency_bands. [Accessed 16 October 2020].

[14] J. S. Subirana, J. J. Zornoza and M. Hernandez-Pajares, “ESA Navipedia,” University of Catalunia, Spain., 2011. [Online]. Available: https://gssc.esa.int/navipedia/index.php/GNSS_signal#:~:text=The%20GNSS%20

satellites%20continuously%20transmit,satellite%20coordinates%20at%20any%20epoch.):. [Accessed 16 October 2020].

[15] ESA, “GNSS signal,” [Online]. Available: https://gssc.esa.int/navipedia/index.php/GNSS_signal#:~:text=The%20GNSS%20satellites%20continuously%20transmit,satellite%20coordinates%20at%20any%20epoch.. [Accessed 15 September 2020].

[16] Liège University , “The erroneous GPS signal,” 2007. [Online]. Available: http://www.reflexions.uliege.be/cms/c_358355/en/the-erroneous-gps-signal?part=2. [Accessed 10 October 2020].

[17] I. R. Webster, “A regional model for the prediction of ionospheric delay for single frequency users of the global positioning system,” 1993.

[18] Y. Zhang, 1. Yang Liu, J. Mei, C. Zhang and J. Wang, “A Study on the Characteristics of the Ionospheric Gradient under Geomagnetic Perturbations,” Sensors, Basel, 2020.

[19] G. S. Rao and G. S. Kumar, “GPS Signal Short-Term Propagation Characteristics Modeling in Urban Areas for Precise Navigation Applications,” 2013.

[20] A. El-Rabbany, Introduction to GPS The Global Positioning System, 2002.

[21] Geospatial Education Platform, “Dilution of Precision,” 17 January 2016. [Online]. Available: https://www.polyu.edu.hk/proj/gef/index.php/glossary/dilution-of-precision/. [Accessed 16 October 2020].

[22] Skybrary, “Ground Based Augmentation System (GBAS),” 2 August 2017. [Online]. Available: https://www.skybrary.aero/index.php/Ground_Based_Augmentation_System_(GBAS. [Accessed 30 October 2020].

[23] Skybrary, “GBAS Landing System (GLS),” 10 September 2017. [Online]. Available: https://www.skybrary.aero/index.php/GBAS_Landing_System_(GLS). [Accessed 30 October 2020].

[24] Federal Aviation Administration (FAA), “Satellite Navigation - GBAS - How It Works,” 21 November 2016. [Online]. Available: https://www.faa.gov/about/office_org/headquarters_offices/ato/service_units/techops/navservices/gnss/laas/howitworks/. [Accessed 31 November 2020].

[25] ESA, “GBAS Fundamentals,” 2011. [Online]. Available: https://gssc.esa.int/navipedia/index.php/GBAS_Fundamentals. [Accessed 31 October 2020].

[26] M.-S. Circiu, M. Felux, M. Caamano and D. Gerbeth, “The Ground Based Augmentation System for Civil Aviation: a Review,” 2017.

[27] Organisation International Civil Aviation, Guide For Ground Based Augmentation, 2013.

[28] ICAO, Guide for Ground Based Augmentation System Implementation, 2013, p. 5.

[29] ICAO, Aeronautical Telecommunications Annex 10, Quebec, 2018

[30] F. Corraro, U. Ciniglio, C. Pasquale and L. Garbarino, An EGNOS Based Navigation System for Highly Reliable Aircraft Automatic Landing, 2009.

[31] R. Sabatini, T. Moore and S. Ramasamy, Global Navigation Satellite Systems Performance Analysis and Augmentation Strategies in Aviation, 2017.

[32] DLR, "ATRA, Neue Dimensionen in der Luftfahrtforschung," Köln, 2016.

[33] PEGASUS, "Software User Manual," 16 January 2004. [Online]. Available: https://www.icao.int/Meetings/AMC/MA/2004/GNSS/sum.pdf. [Accessed 13 December 2020].